Environ Monit Assess (2025) 197:683
https://doi.org/10.1007/s10661-025-14118-y

RESEARCH

Combined effects of land use and geology on potentially toxic elements contamination in lacustrine sediments from the Araguaia River floodplain, Brazilian Savanna

Lucas Cabrera Monteiro · Ludgero Cardoso Galli Vieira · José Vicente Elias Bernardi · Thiago Aluisio Maciel Pereira · Walkimar Aleixo da Costa Júnior · Wesley Pinheiro da Silva · Leonardo Almeida Guerra dos Santos · José Francisco Gonçalves Júnior · João Carlos Nabout · José Alexandre Felizola Diniz Filho · Jeremie Garnier · Cleber Lopes Filomeno · Ronaldo de Almeida · Wanderley Rodrigues Bastos

Received: 16 February 2025 / Accepted: 11 May 2025 / Published online: 27 May 2025

Abstract Freshwater ecosystems play a fundamental role in maintaining biodiversity and supporting human societies; however, the mobilization of potentially toxic elements (PTEs) poses a significant threat to their integrity. Here, we characterized the elemental composition of the bottom sediments of 72 lakes in the Araguaia River floodplain, a region that has been undergoing large-scale environmental degradation due to the advance of anthropogenic activities. The objectives of this study were to assess the degree of Cr, Cu, Ni, Pb, and Zn contamination in bottom sediments, identify critically contaminated areas, and evaluate the contribution of anthropogenic and natural factors to the distribution of PTEs in the floodplain. The contamination and enrichment factors followed the order of Ni > Cr > Pb > Cu > Zn. Notably, Ni and Cr showed the highest proportions of samples with moderate and significant enrichment, respectively, with a considerable and very high degree of contamination. Critical areas of PTE contamination have been identified in lakes with intense anthropogenic land use and igneous and metamorphic rocks derived from mafic parent materials. All PTEs

Supplementary Information The online version contains supplementary material available at https://doi.org/10.1007/s10661-025-14118-y.

L. C. Monteiro (✉)
Graduate Program in Ecology, Institute of Biological Sciences, University of Brasília, Brasília, DF, Brazil
e-mail: lcabreramonteiro@gmail.com; cabrera.lucas@aluno.unb.br

L. C. Monteiro · L. C. G. Vieira
Center for Environmental and Limnological Studies and Research, University of Brasília, Planaltina, DF, Brazil
e-mail: ludgero@unb.br

L. C. Monteiro · J. V. E. Bernardi
Laboratory of Geostatistics and Geodesy, University of Brasília, Planaltina, DF, Brazil
e-mail: bernardi@unb.br

T. A. M. Pereira
Graduate Program in Chemistry, Institute of Chemistry, University of Brasília, Brasília, DF, Brazil
e-mail: thiagomaciel6198@gmail.com

T. A. M. Pereira · W. A. da Costa Júnior · R. de Almeida · W. R. Bastos
Laboratory of Environmental Biogeochemistry Wolfgang Christian Pfeiffer, Federal University of Rondônia, Porto Velho, RO, Brazil
e-mail: walkimarcosta@gmail.com

R. de Almeida
e-mail: ronaldoalmeida@unir.br

W. R. Bastos
e-mail: bastoswr@unir.br

W. P. da Silva
Graduate Program in Environmental Sciences, University of Brasília, Planaltina, DF, Brazil
e-mail: wesleyps2008@gmail.com

were strongly correlated with the Mg concentrations in the sediments, which were used here as a proxy for regional geology characterization. Land-use intensity was positively associated with higher Cr and Ni concentrations in sediments. Organic matter content significantly influenced the accumulation of PTEs in sediments (except for Cr). This study offers valuable insights into the sources, distribution, and control of PTE contamination in floodplain lakes, underscoring the importance of sustainable land use management in mitigating contamination risks.

Keywords Contamination factor · Pollution load index · Source apportionment · Mafic rock · Cerrado

Introduction

Freshwater ecosystems play a vital role in maintaining biodiversity and supporting human society. However, despite their ecological significance, these ecosystems cover only a small portion of the Earth's surface and are increasingly under anthropogenic pressure. Among the various effects of human activities, contamination by potentially toxic elements (PTEs) is of particular concern (Carvalho et al., 2022). PTEs occur naturally in the Earth's crust and are mobilized into aquatic ecosystems through processes such as volcanic eruptions and rock weathering (Kapoor & Singh, 2021). Nonetheless, anthropogenic emissions have vastly exceeded natural mobilization rates, significantly altering the distribution of PTEs across environmental compartments, primarily through mining, industrial activities, and the discharge of urban waste and effluents (Andrade et al., 2018; Hanfi et al., 2020; Yu et al., 2021). Additionally, the intensification of agricultural activities in river basins represents a diffuse source of PTE mobilization (Ochoa-Contreras et al., 2023; Rosolen et al., 2015), especially in regions with soils derived from mafic and metavolcanic rocks, which are inherently rich in PTEs (Quaresma et al., 2022).

In aquatic ecosystems, PTEs are deposited in sediments through complex interactions involving sedimentation, adsorption, and co-precipitation (Yao & Gao, 2007). These interactions are more complex in floodplain lakes, where seasonal flood pulses influence sediment input rates and redox conditions (van Griethuysen et al., 2005). PTEs bound to particulate matter from rivers, terrestrial ecosystems, and atmospheric deposition are transported through the water column. While larger particles settle rapidly, finer and colloidal particles remain suspended for longer, with flocculation driven by dissolved organic matter, which promotes sedimentation (Donohue & Garcia Molinos, 2009; Plach et al., 2011). Dissolved and colloidal PTE fractions in the water column are adsorbed onto humic substances, clay minerals, and iron and manganese oxyhydroxides through cation exchange and electrostatic reactions (Li et al., 2018, 2023; Ruello et al., 2011), forming insoluble compounds that precipitate in the bottom sediments (López et al., 2010; Yuan et al., 2014). These processes are regulated by water and sediment physicochemical parameters such as redox potential, suspended sediment concentrations, and organic matter content (Khan et al., 2016; Ponting et al., 2021; Sadeghi et al., 2012). Consequently, bottom sediments can act as temporary reservoirs or sources of PTEs, depending on environmental conditions.

L. A. G. dos Santos
Laboratory of Metacommunity and Landscape Ecology, Institute of Biological Sciences, Universidade Federal de Goiás, Goiânia, GO, Brazil
e-mail: leonardoalmeida1999@hotmail.com

J. F. Gonçalves Júnior
AquaRiparia/Laboratory of Limnology, Institute of Biological Sciences, University of Brasília, Brasília, DF, Brazil
e-mail: jfjunior@unb.br

J. C. Nabout
State University of Goiás, Anápolis, GO, Brazil
e-mail: joao.nabout@ueg.br

J. A. F. Diniz Filho
Department of Ecology and Evolution, Institute of Biological Sciences, Universidade Federal de Goiás, Goiânia, GO, Brazil
e-mail: diniz@ufg.br

J. Garnier
Institute of Geosciences, University of Brasília, Brasília, DF, Brazil
e-mail: garnier@unb.br

C. L. Filomeno
Analytical Center, Institute of Chemistry, University of Brasília, Brasília, DF, Brazil
e-mail: cleber.filomeno@gmail.com

Elements such as chromium (Cr), copper (Cu), nickel (Ni), and zinc (Zn) play various roles in aquatic ecosystems but have different degrees of toxicity, depending on their concentrations, chemical form, and bioavailability, affecting both biological communities and human health (Kou et al., 2024; Sigel & Sigel, 2019; Vandeuren et al., 2023). For example, trivalent chromium (Cr (III)) is essential for the metabolism of proteins, fats, and carbohydrates (Swaroop et al., 2019), whereas hexavalent chromium (Cr (VI)) is a known carcinogen (IARC, 2012). Conversely, lead (Pb) has no biological function and is toxic, even at low concentrations (Kumar et al., 2020). Understanding the processes governing the transport and fate of PTEs in aquatic ecosystems is critical for assessing their potential risks to ecosystem integrity and human health.

Analyzing PTE concentrations in bottom sediments enables identification of their origins, spatial distributions, and associated contamination risks (Basti et al., 2025; Tepe et al., 2022; Zhang et al., 2019). Various quality guidelines and indices have been developed to assess sediment contamination, with wide applications in evaluating the extent of pollution in aquatic ecosystem (CCME, 2003; Ferreira et al., 2022). For instance, the contamination factor (Hakanson, 1980) and enrichment factor (Sutherland, 2000) enable the assessment of individual levels of contamination in lake sediments, while the pollution load index provides an integrated assessment of multiple pollutants (Tomlinson et al., 1980). Combining sediment assessment indices with spatial analysis has proven effective in identifying priority areas for contamination at both local and regional scales (Monteiro et al., 2023; Sojka et al., 2022). Such assessments are particularly crucial for ecosystems experiencing large-scale environmental degradation due to advancing anthropogenic activities.

The Araguaia River floodplain, located in the Brazilian savannah (*Cerrado* biome), has undergone significant land-use changes since the 1970 s (Pelicice et al., 2021). Intense deforestation has significantly altered hydrological and geomorphological processes in the Araguaia River (Latrubesse et al., 2009; Teixeira et al., 2024), affecting the transport of Hg (Monteiro et al., 2023) and pesticides (Lima-Junior et al., 2024) into aquatic ecosystems. Furthermore, Moraes et al. (2023) demonstrated that the combined effects of land use and the occurrence of igneous rocks in the sub-basins increased Hg concentrations in the lake sediments of the Araguaia River floodplain. However, data on the concentrations and factors influencing the distribution of other PTEs in Araguaia floodplain lakes remain scarce. In this context, we characterized the elemental composition of bottom sediments from 72 floodplain lakes, focusing on PTEs Cr, Cu, Ni, Pb, and Zn. Our study aimed to address the following questions: (i) What is the degree of PTE contamination in the sediments? (ii) How are PTE concentrations spatially distributed, and what are the critical contamination areas? (iii) How do land-use intensity, water physicochemical parameters, sediment organic matter content, and regional geology influence PTE concentrations? Additionally, we analyzed the elemental composition of the rock samples to trace the origins and transport of PTEs to the bottom sediments. These findings provide an integrated assessment of the natural and anthropogenic factors controlling PTE contamination and distribution in a large floodplain, highlighting elements that exceed quality guidelines and identifying priority areas for monitoring.

Material and methods

Study area

The Araguaia River is a large river located predominantly in the *Cerrado* biome in the Center-West region of Brazil. Draining from south to north, between the states of Goiás, Mato Grosso, Tocantins, and Pará, the Araguaia River has an average flow of 6420 $m^3\ s^{-1}$ and a drainage area of 377,000 km^2 (Latrubesse & Stevaux, 2002). A tropical climate with a dry winter (Aw) is predominant in the river basin, with a rainy season from October to April and a dry season from May to September. The Middle Araguaia stretch is characterized by an alluvial plain with a low amplitude of fluctuations in the water level (Junk et al., 2014), with an average annual flow ranging from 1175 $m^3\ s^{-1}$ at the most upstream monitoring station to 5283 $m^3\ s^{-1}$ at the most downstream station (Aquino et al., 2009). The floodplain is mainly composed of terraces and quaternary alluvial deposits of the Araguaia Formation, with the occurrence of mafic and ultramafic minerals in the sub-basins of the right bank tributaries, such as amphibolite, basalt,

gabbro, metagabbro, serpentinite, orthogneiss, pyroxenite, peridotite, and talc schist (CPRM, 2004).

Middle Araguaia has predominantly pasture and agricultural land use to the south (upstream), and a mosaic of preserved areas to the north (downstream), which is home to wetlands of international importance for biodiversity conservation, including Bananal Island (Ramsar site) (Fig. 1). Despite their negligible proportions on a regional scale, copper (Cu) mining and human settlements can represent a source of diffuse pollution on a local scale. Cu mining is in the Crixás-Açú River sub-basin, 45 km from the river channel and 150 km upstream of the nearest sampling unit. The municipalities in our study area are predominantly rural, with urban areas varying between 0.9 and 8 km^2 and population density between 0.4 and 3.9 inhabitants/km^2 (IBGE, 2022). Despite the low level of economic development in the towns, the tourism industry stands out in Middle Araguaia, with a significant increase in the local population during the low-water period.

Sediment sampling, processing, and determination of the elemental composition

Bottom sediment samples were collected during the high-water period (February 2023) in 72 floodplain lakes connected to the Araguaia River (n = 39) and four tributaries: Água Limpa Stream (n = 5), Vermelho River (n = 14), Peixe River (n = 11), and

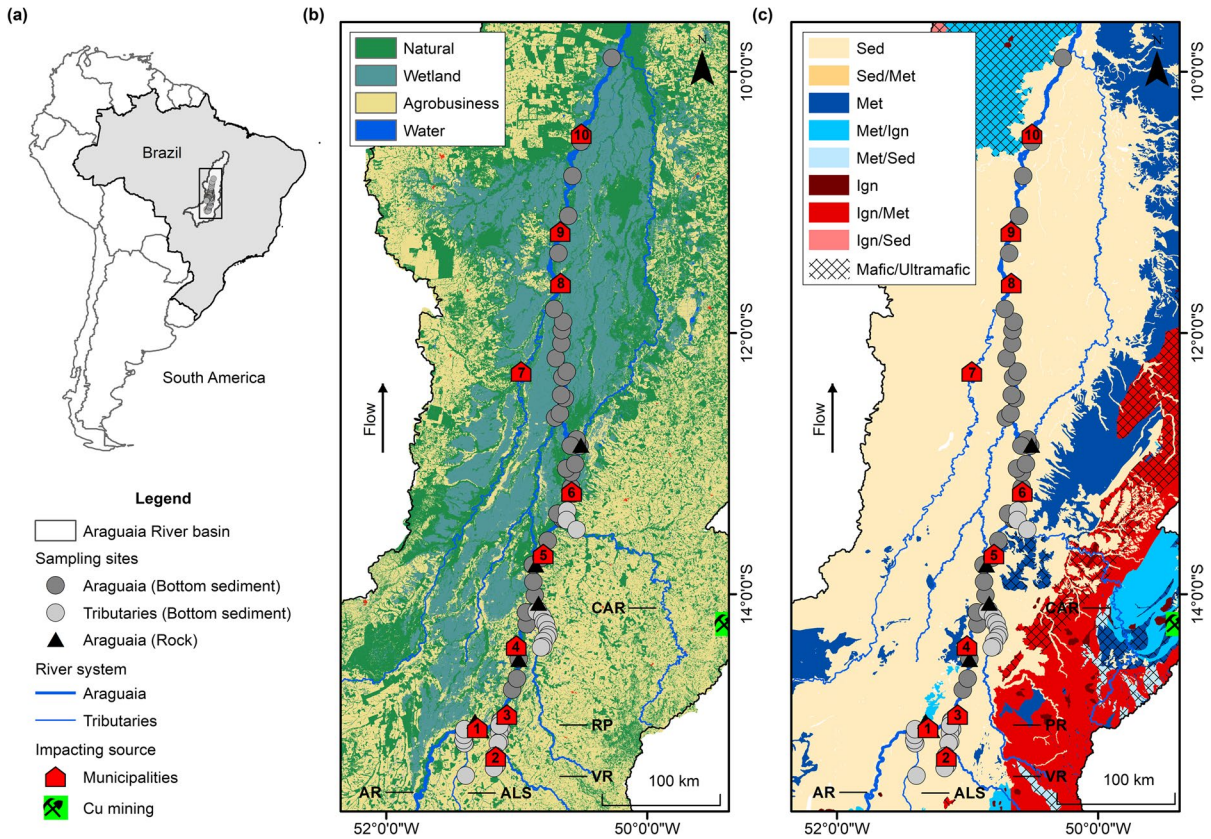

Fig. 1 **a** Map of Brazil and location of the study area, highlighting **b** land use and occupation and **c** geology. **b** The "Natural" class comprises forest, savannah, and grassland formations, and the "Agrobusiness" class comprises areas destined for pasture, agriculture, and forestry. **c** The acronyms in the legend indicate the rock formation process: Sed, sedimentary rocks; Met, metamorphic rocks; and Ign, igneous rocks. Cross-hatching lines indicate the presence of minerals derived from mafic and ultramafic parent materials. The acronyms in figures **b** and **c** represent the names of the rivers: AR, Araguaia River; ALS, Água Limpa Stream; VR, Vermelho River; PR, Peixe River; and CAR, Crixás-Açú River. The numbers indicate the municipalities and districts: (1) Itacaiú; (2) Britânia; (3) Aruanã; (4) Cocalinho; (5) São José dos Bandeirantes; (6) Luiz Alves do Araguaia; (7) Novo Santo Antônio; (8) São Félix do Araguaia; (9) Luciara; and (10) Santa Terezinha

Crixás-Açú River ($n = 3$) (Fig. 1). Sediment samples were collected with an Eckman dredge (~ 10 cm), stored in polyethylene bags, and transported in thermal boxes with ice. In the laboratory, the sediment samples were air-dried in a clean environment (25–30 °C), ground using an electric mortar and pestle, and sieved (125 µm).

Chemical extraction for the quantification of the selected elements (Al, Ba, Cr, Cu, Fe, Mg, Mn, Ni, Pb, Ti, and Zn) was carried out using an open system, using an alternative method equivalent to that in the U.S. EPA 3051 (U.S. EPA, 1996). Initially, 8 mL of 65% nitric acid (HNO_3) was added, and the samples were transferred to a hotplate at 120 °C for evaporation. Next, 8 mL of a mixture of HCl and HNO_3 (3:1, v/v) was added, and the samples were returned to the hotplate until evaporation. The samples were resuspended with hydrochloric acid (0.1 N HCl), filtered through paper filters (3-µm pore size), and the final volume was completed with ultrapure water (Milli-Q Plus, Millipore, Bedford, USA). The total concentrations of the elements were quantified using inductively coupled plasma optical emission spectrometry (ICP-OES Optima 8300, Perkin Elmer, Waltham, USA). Analytical quality control was performed by analyzing blank samples (reagents and filters only) and the certified reference material EnviroMAT SS2 (SCP Science, Quebec, Canada), with mean recovery rates between 88 and 110%.

Rock sampling, processing and determination of the elemental composition

Samples of rocky outcrops ($n = 9$) and pebbles ($n = 2$) were collected from the Araguaia River Channel during the rising water period in November 2021 and November 2023 (Fig. 1). The samples were air-dried and pulverized in a pan mill. The semi-quantitative determination of major oxides was carried out by energy dispersive X-ray fluorescence spectrometry (ED-XRF) using Shimadzu EDX720HS equipment (Shimadzu Corporation, Kyoto, Japan). The accuracy of the analytical method was determined by the sum of the proportions of each oxide identified and the result of the mass loss by ignition (450 °C for 4 h), with a total proportion between 95 and 107%. Chemical extraction for the quantification of the selected elements (Al, Ba, Cr, Cu, Fe, Mg, Mn, Pb, Ti, and Zn) was performed using alkaline fusion with lithium metaborate at 950 °C for 30 min. Subsequently, 50 mL of hydrochloric acid (2 M HCl) was added, and the samples were mixed in a magnetic stirrer to dilute the fusion product. The total element concentrations were quantified using inductively coupled plasma optical emission spectrometry (ICP-OES, Agilent 5100, Agilent Technologies, Santa Clara, USA). The internal reference material BG-1 produced by the Geochemistry Laboratory (University of Brasilia, Brazil) was used to evaluate the accuracy of the analytical method, with mean recovery rates between 85 and 111%.

Pollution assessment of potentially toxic elements in bottom sediments

The concentrations of Cr, Cu, Ni, Pb, and Zn in the sediments were compared with the threshold effect level (TEL) and probable effect level (PEL) established by the sediment quality guidelines (SQG) of the Canadian Council of Ministers of the Environment (CCME, 2003) and adopted by the Brazilian government (Brazil, 2012). The TEL represents the threshold below which there is the lowest probability of adverse effects on biota, whereas the PEL indicates the threshold above which there is the highest probability of adverse effects on biota.

The contamination factor (CF) was used to assess the degree of contamination of each element concerning the regional reference concentration (Hakanson, 1980). CF was calculated using Eq. 1, where C_n is the concentration of a given element in each sampling unit and C_b is the reference concentration. CF results were grouped into four degrees of contamination: no contamination ($CF < 1$), moderate ($1 \leq CF \leq 3$), considerable ($3 \leq CF \leq 6$), and high ($CF > 6$) (Hakanson, 1980).

$$CF = C_n / C_b \quad (1)$$

The enrichment factor (EF) was used to assess the degree of enrichment of the concentrations of the selected PTEs in relation to a conservative element. Aluminum was selected as a conservative element because it has low mobility in sediments (Boës et al., 2011) and shows less variability compared to other elements commonly used to calculate the EF, such as Fe and Ti. The normalization of PTE concentrations by Al is important to compensate for the

granulometric and mineralogical variation of samples between sampling units (Wang et al., 2015). However, Al-normalized concentrations do not consider uncertainties and randomness in aquatic ecosystems because of the physicochemical parameters of the water and anthropogenic inputs on a local scale (Li et al., 2021). Thus, the integration of CF and EF allows for a robust assessment of the degree of individual contamination by PTEs in the bottom sediments. EF was calculated using the ratio of the concentrations of each selected element (C_n) to Al (C_{Al}) at each sampling site and the ratio of the regional reference concentrations (Eq. 2; Sutherland, 2000). The EF results indicated five degrees of enrichment: minimal (EF <2), moderate ($2 \leq$EF <5), significant ($5 \leq$EF <20), very high ($20 \leq$EF <40), and extremely high (EF ≥ 40) (Sutherland, 2000).

$$\mathrm{EF} = \frac{\left(C_n/C_{\mathrm{Al}}\right)_{\mathrm{local}}}{\left(C_n/C_{\mathrm{Al}}\right)_{\mathrm{background}}} \quad (2)$$

The pollutant load index (PLI) was applied to the integrated assessment of contamination for the entire set of potentially toxic elements at each sampling site. The PLI was calculated using Eq. 3, where CF is the contamination factor for each selected element (Tomlinson et al., 1980). PLI values <1 indicate that the concentrations agree with the geochemical baseline, whereas PLI values >1 indicate enrichment of the concentrations by anthropogenic sources.

$$\mathrm{PLI} = \left(\mathrm{CF_{Cr}} \times \mathrm{CF_{Cu}} \times \mathrm{CF_{Ni}} \times \mathrm{CF_{Pb}} \times \mathrm{CF_{Zn}}\right)^{\frac{1}{5}} \quad (3)$$

Considering that there are no previous studies on PTE concentrations in the Araguaia River floodplain, we calculated regional background concentrations from our dataset. The sampling sites were separated into three groups based on the river system: (i) tributaries, (ii) Araguaia upstream of Bananal Island, and (iii) Araguaia on Bananal Island. The groups were defined a priori to ensure the representativeness of the natural areas between the sections of the Araguaia River and its tributaries owing to the predominance of natural areas on Bananal Island. The sampling sites with the highest proportion of natural areas (forest, savannah, grassland, and wetland formations) in each group were selected to calculate the reference values ($n = 27$). We then used the median absolute deviation (MAD) method to identify the upper limit of the regional background and remove geochemical outliers for each chemical element (Eq. 4; Reimann et al., 2005). After removing concentrations above the upper limit, the regional reference value was calculated using the median of the remaining sampling units (Carrillo et al., 2022).

$$\begin{aligned} \mathrm{MAD} &= \mathrm{Median}\left(\left|X_i - \mathrm{Median}(X)\right|\right), \\ \text{Upper Threshold} &= \mathrm{Median} + (2 \times \mathrm{MAD}) \end{aligned} \quad (4)$$

Assessment of the spatial structure and identification of hotspots contamination in sediments

Variographic analysis was applied to assess the contribution of endogenous and exogenous factors to the spatial dependence of the PTEs. Endogenous factors represent the structural characteristics of bottom sediments, including mineral composition, physicochemical parameters, and geological formations (Angelini et al., 2016; Dong et al., 2024). However, exogenous factors indicate conditions external to the variable studied, such as variations in environmental conditions and anthropogenic influences (Angelini et al., 2016; Monteiro et al., 2024a). The variogram combines the nugget (C_0), sill (C), and amplitude (a) to model how the similarity between sampling sites decreases with increasing distance (h) (Goovaerts, 1997). The nugget represents the small-scale variance, the sill indicates the total variance, and the amplitude is the distance at which the spatial correlation becomes random. Spatial dependence was calculated as the ratio between nugget and sill, classified as strong, $<25\%$; moderate, 26–75%; and weak, $>76\%$ (Cambardella et al., 1994). Considering that spatial dependence is mainly promoted by endogenous factors (Dale & Fortin, 2014), strong spatial dependence indicates the predominance of endogenous factors for the distribution of PTEs in bottom sediments, whereas weak spatial dependence suggests the predominance of exogenous factors. The experimental variograms were adjusted with the indicator kriging method using the Geostatistical Wizard function of ArcMap 10.8.1 software (Esri, Redlands, USA). The best models were selected based on the mean error (ME $\cong 0$) and the standardized root mean squared scaled error (RMSSE $\cong 1$) of the probability predictions.

The Getis-Ord (Gi*) statistic was used to cluster extreme values and identify critical areas (hotspots) for individual (CF) and integrated (PLI) contamination of PTEs in bottom sediments on a local scale. The Gi* method measures the degree of local autocorrelation of a given variable in a site with respect to neighboring sampling sites by comparing the sum of the values of the weighted points located within a certain radius of the original weighted point with the sum of all the values in the dataset (Getis & Ord, 2010). The global Moran's index was applied beforehand to check the magnitude of the global autocorrelation in our dataset (*spdep* package; R Core Team, 2024). Global autocorrelation was significant for all PTEs (Table S1), biasing the significance tests on a local scale (Sokal et al., 1998). Therefore, Gi* was used to assess the clustering of the sampling sites using an exploratory approach. Gi* was calculated using the hot spot analysis function in ArcMap 10.8.1 software.

Characterization of environmental variables

The oxidation–reduction potential (ORP), total dissolved solids (TDS), electrical conductivity (Ec), turbidity, and depth were measured in situ using a multiparameter probe (U-50, Horiba, Kyoto, Japan). The water transparency was measured using a Secchi disk. Water samples were collected from the subsurface in polyethylene bottles and stored in a thermal box with ice. On the same day that the samples were collected, some of them were filtered using glass microfiber membranes (Whatman GF/C, Cytiva, Amersham, UK). The unfiltered samples were used to determine the total phosphorus, whereas the concentrations of phosphate, nitrate, and ammoniacal nitrogen were measured from the filtered samples. The total phosphorus, phosphate, nitrate, and ammoniacal nitrogen concentrations were determined using spectrophotometry. Total phosphorus and phosphate levels were determined using the ascorbic acid method. Nitrate and ammoniacal nitrogen concentrations were determined using the cadmium reduction and salicylate methods, respectively (APHA, 2005). Zero values were assigned to the samples with concentrations below the detection limit.

The sediment organic matter (SOM) content was estimated by loss on ignition (LOI) by heating 1.5 g of each sample (in duplicate) in a muffle furnace at 500 °C for 4 h. We used Mg concentrations as a proxy for the occurrence of geogenic mobilization sources because mafic rocks or sedimentary and metamorphic rocks derived from mafic materials have high concentrations of Mg, Cr, Cu, and Ni (Alloway, 1990; Lipp et al., 2020). The Mg quantification method and analytical quality control are described in the "Sediment sampling, processing, and determination of the elemental composition" section.

Land-use and land-cover data were obtained from the MapBiomas Project with a spatial resolution of 30 m (MapBiomas Project, 2024). The characterization of land use and land cover was carried out in 10-km buffers from the collection point of each lake. The land-use classes were grouped into forest formations, savannah formations, grassland formations, wetlands, agrobusiness (pasture, agriculture, and forestry), urban areas, mining, other non-vegetated areas, and water bodies. The absence of urban areas was detected around most lakes (77%), so the land use index (LUI) was used to provide a continuous variable representing the combined impact of agricultural activities and urban areas (Eq. 5, Rawer-Jost et al., 2004).

$$\mathrm{LUI} = 4 \times \%\mathrm{Urban\ areas} + 2 \times \%\mathrm{Agrobusiness} \quad (5)$$

To assess the influence of mining on the concentration of PTEs in the sediments, we selected only lakes associated with the Crixás-Açú River and the Araguaia River (downstream of the Crixás-Açú River). The locations of the metallic mining areas were obtained from the MapBiomas Project (MapBiomas Project, 2024), and the Euclidean distance from each sampling unit to the nearest Cu mining area upstream was calculated using the Near tool in ArcMap 10.8.2 software. For statistical analyses, the distances were transformed into semi-quantitative data: (1) 150–200 km; (2) > 200 km; (3) > 300 km; and (4) no occurrence of upstream mining.

Modeling multivariate patterns of PTEs distribution

We used principal component analysis (PCA) to explore the dissimilarity of the elemental ratios (element/Al) of the rocks collected in the main channel of the Araguaia River and in the lake-bottom sediments (*rda* function). The Kaiser–Meyer–Olkin criterion (KMO = 0.77) and Bartletts test of sphericity

($\chi^2(28) = 765.72$; $p < 0.001$) were used to confirm the suitability of our dataset for PCA. Spearman's non-parametric correlation (r_s) was applied to assess whether the concentrations of PTEs in bottom sediments vary in a similar way in the sampling sites (*cor* function). Positive correlations indicate that the PTEs are similar in terms of the source of mobilization and geochemical behavior (Ustaoğlu & Islan, 2020; Basti et al., 2025). In addition, hierarchical cluster analysis (HCA) was used to assess the dissimilarity of elements related to the sources of mobilization. HCA was performed using Euclidean distance and the unweighted pair group method using arithmetic averages (UPGMA) (*hclust* function). The variables were standardized with mean zero and standard deviation one (*decostand* function), and the cophenetic correlation coefficient (ccc) was used to measure the fit between the dendrogram and distance matrix.

Generalized linear mixed models (GLMM) were used to assess the relative contribution of land use and occupation classes, physico-chemical water parameters, organic matter, and Mg content in sediments (fixed effects), and the concentrations of Cr, Cu, Ni, Pb, and Zn in bottom sediments (response variables). The sub-basins were included as random effects to assess the influence of the specific characteristics of each river system and the land use in its drainage area on the distribution of the elements. The predictor variables were selected using the forward selection method (*regsubsets* function). Descriptive statistics for all candidate predictor variables are available in the Supplementary Information (Table S2). GLMMs were estimated using the restricted maximum likelihood (REML) approach (*lmer* function). The adjusted coefficient of determination (R^2) was obtained using the *r*.squaredGLMM function, providing two values: conditional R^2 (R^2_c), which represents the total variance explained by random fixed effects, and marginal R^2 (R^2_m), which represents the variance explained by the fixed effects. The overall significance of the models was calculated using the likelihood ratio test (LRT) between the final model for each potentially toxic element and a null model (*lrtest* function). The relative contribution of each predictor variable (fixed effects) was obtained by hierarchical partitioning of the marginal R^2 ($R^2_{m\text{-partial}}$) (*glmm.hp* function).

The proportion of land-use classes and organic matter content was converted by the square root of the arcsine. The other variables, except for distance to Cu mining and LUI, were log-transformed. The residuals were evaluated for normality (*ks.test* function), homoscedasticity (*testDispersion* function), and autocorrelation (*moran.test* function). These assumptions were not violated. The analyses were carried out in the R programming environment (R Core Team, 2024) using the packages *stats*, *vegan*, *EFAtools, leaps*, *lme4*, *DHARMa*, *lmetest*, *MuMIn*, *glmm.hp*, and *spdep*.

Results

Elemental composition of bottom sediment and rock samples

The mean concentrations of the chemical elements in the bottom sediments followed the order Fe > Al > Mg > Mn > Cr > Ba > Zn > Ti > Pb > Ni > Cu (Table 1). The mean concentrations in the rocks followed the order of Al > Fe > Mg > Ti > Ba > Mn > Zn > Cr > Cu (Table 1). Pb concentrations were below the detection limit for all rock samples. The main oxides in the rock samples were SiO_2 (39.4–96.9%), Al_2O_3 (2.4–17.9%), and Fe_2O_3 (0.1–6.1%). The first two axes of the principal component analysis explain 74% of the variability in the elemental ratios, indicating a clear separation between the compositions of the rock and sediment samples (Fig. 2). All elemental ratios were negatively correlated with axis 1. The elemental ratios of Ti, Ba, Cu, and Fe were positively correlated with axis 2, mainly associated with the rock samples, whereas the elemental ratios of Cr, Mg, Mn, and Zn were associated with the bottom sediment samples and negatively correlated with axis 2. The complete composition of the rock oxides and elemental ratios of the rocks and sediments are available in the Supplementary Information (Tables S3 and S4).

Assessing the contamination of PTEs in bottom sediments

The bottom sediment samples showed concentrations mostly above the regional background concentrations, except for Cu, with Ni, Zn, and Pb standing out (Table 2). The regional background concentrations were consistently lower than the threshold effect level (TEL) and probable effect level (PEL), except for Cr, whose background concentration was 3.5 times

Table 1 Elemental composition of the bottom sediment and rock samples (mg kg^{-1}). *SD*, standard deviation; *CV*, coefficient of variation

Bottom sediment ($n=72$)	Al	Ba	Cr	Cu	Fe	Mg	Mn	Ni	Pb	Ti	Zn
Mean	12,964	111	172.6	12.2	20,949	1493	537.8	18.8	24.7	43	44.6
Median	13,574	122.2	137.8	10.9	19,253	1448	510.4	15.6	27.4	33.3	46.2
SD	5396	39.9	98.4	8	13,227	825	475	15	11.6	49.1	13.6
Minimum	2864	12.8	28.8	1.7	1305	86.2	3.9	1.5	2.4	3.4	9.5
Maximum	26,391	196.4	448.7	59.1	60,104	3927	2935	92.4	50	397.1	76.7
CV (%)	42	36	57	66	63	55	88	80	47	114	31
Rocks ($n=11$)											
Mean	42,890	519.2	46.9	34.3	33,886	1079	304.4	NA	< LOD	1042	54
Median	41,964	327.6	41.7	38.3	15,165	391.7	165.7	NA	< LOD	889.2	43.9
SD	17,473	467.5	25.1	12.6	61,196	1374	334.2	NA	< LOD	846.4	36
Minimum	807.5	186.9	24.2	14.1	8573	60.2	44.9	NA	< LOD	72.4	7.3
Maximum	68,606	1,741	116.6	48.4	21,801	3988	1019	NA	< LOD	2745	116.4
CV (%)	41	90	53	37	181	127	110	NA	< LOD	81	67

< LOD, concentrations below the detection limit; ***NA***, Ni concentrations were not quantified in the rocks

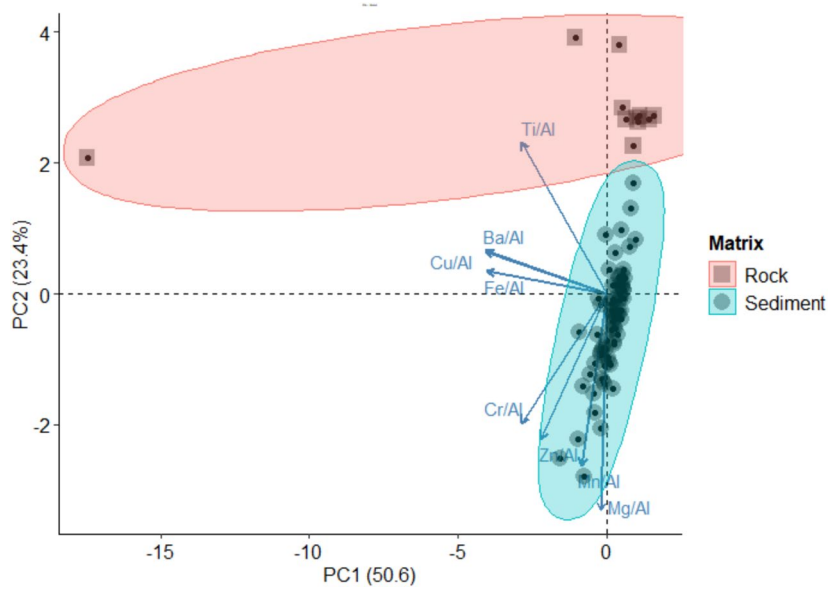

Fig. 2 Bivariate plots representing the order of elemental ratios of the sediment and rock samples using principal component analysis

higher than that of the TEL. Only one sampling site had a Cr concentration below the values established by the sediment quality guidelines, with concentrations above the PEL in 83.3% of the samples. In contrast, the concentrations of the other elements were mostly below the TEL, with concentrations between the TEL and PEL values for Ni and Pb and above the PEL for Ni (Table 2).

The contamination factor (CF) and enrichment factor (EF) followed the order Ni > Cr > Pb > Cu > Zn (Table 2). Only Cu exhibited a low degree of contamination (CF < 1). In general, more than half of the sampling sites showed moderate contamination (1 ≤ CF ≤ 3), mainly of Pb and Zn. Considerable levels of contamination (3 ≤ CF ≤ 6) were determined for Ni, Cr, and Cu, whereas only one sampling site showed very high contamination by Ni (CF > 6). Considering the Al-normalized concentrations, the bottom sediments showed minimal degrees of enrichment at most sampling sites (EF < 2). The

Table 2 The average concentrations of Cr, Cu, Ni, Pb, and Zn were compared with regional background concentrations, sediment quality guideline limits, contamination factors, and enrichment factors

	Cr	Cu	Ni	Pb	Zn
Mean concentration (mg kg^{-1})	172.6 ± 98.4	12.2 ± 8	18.8 ± 15	24.7 ± 11.6	44.6 ± 13.6
Regional background (mg kg^{-1})	132.9	11.5	12.0	22.9	42.8
Threshold effect level (mg kg^{-1})	37.3	35.7	18	35	123
Probable effect level (mg kg^{-1})	90	197	35.9	91.3	315
Contamination factor (unitless)	1.3 ± 0.7	1.1 ± 0.7	1.6 ± 1.2	1.1 ± 0.5	1.0 ± 0,3
Low contamination (*N*; %)	32 (44.4%)	39 (54.2%)	23 (31.9%)	27 (37.5%)	26 (36.1%)
Moderate contamination (*N*; %)	37 (51.4%)	32 (44.4%)	41 (56.9%)	45 (62.5%)	36 (63.9%)
Considerable contamination (*N*; %)	3 (4.2%)	1 (1.4%)	7 (9.8%)	-	-
High contamination (*N*; %)	-	-	1 (1.4%)	-	-
Enrichment factor (unitless)	1.4 ± 0.6	1.1 ± 0.4	1.6 ± 1.5	1.1 ± 0.3	1.2 ± 0.4
Minimal enrichment (*N*; %)	64 (88.9%)	69 (95.8%)	54 (75.0%)	71 (98.6%)	69 (95.8%)
Moderate enrichment (*N*; %)	8 (11.1%)	3 (4.2%)	15 (20.8%)	1 (1.4%)	3 (4.2%)
Significant enrichment (*N*; %)	-	-	3 (4.2%)	-	-

highest degrees of enrichment were observed for Ni, with moderate ($2 \leq EF < 5$) and significant ($5 \leq EF < 20$) enrichments in 20.8% and 4.2% of the samples, respectively. For Cr, 11.1% of the samples showed moderate enrichment. Additionally, considering all the elements assessed, approximately 60% of the sampling sites had a pollution load index greater than one.

Spatial structure and hotspots of PTE contamination in sediments

Variographic analysis showed strong to moderate spatial dependence for Zn and Ni concentrations (18.9% and 29.7%, respectively), indicating the predominant contribution of endogenous factors. The spatial dependence of Cr and Cu concentrations was moderate (42.7% and 43%, respectively), suggesting the contribution of endogenous and exogenous factors, whereas the weak spatial dependence observed for Pb (92.6%) reflects the predominance of exogenous factors (Table S5). The amplitudes of the variograms showed that Cr and Ni concentrations varied over long distances (> 100 km), Cu and Pb concentrations varied over moderate distances (≅ 50 km), and Zn concentrations varied at a local scale (25 km) (Table S5).

Hotspot analysis showed that the elements evaluated had different spatial distribution patterns on a local scale. The Cr and Ni contamination hotspots were determined in the southern region of the floodplain (upstream), mainly in the Água Limpa Stream and Vermelho River (Fig. 3a, c). The Cu contamination hotspots in the bottom sediments were determined in the sampling units with upstream Cu mining located in the Crixás-Açú sub-basin and downstream of the confluence with the Araguaia River (Fig. 3b, g).

The hotspots of Pb and Zn contamination showed a similar pattern, located in the sub-basins of the Água Limpa Stream, Vermelho River, and Crixás-Açú River, as well as lakes situated downstream of the confluence of the Araguaia River with the Peixe River (Fig. 3d, e). No hotspots for any of the elements were determined at the sampling sites located on the Peixe River and Bananal Island. Considering the cumulative contamination factor for all the selected elements, the critical areas for pollution were located in the sub-basins of the Água Limpa Stream, Vermelho River, and Crixás-Açú River, a region with intense land use and the occurrence of igneous and metamorphic rocks (Fig. 3f, g, h).

Local and regional factors controlling the distribution of PTEs in bottom sediments

All PTEs were significantly correlated, especially Cr and Ni ($r_s = 0.84$; $p < 0.0001$), Ni and Pb ($r_s = 0.76$; $p < 0.0001$), and Pb and Cu ($r_s = 0.73$; $p < 0.0001$) (Fig. 4a). Hierarchical cluster analysis indicated a

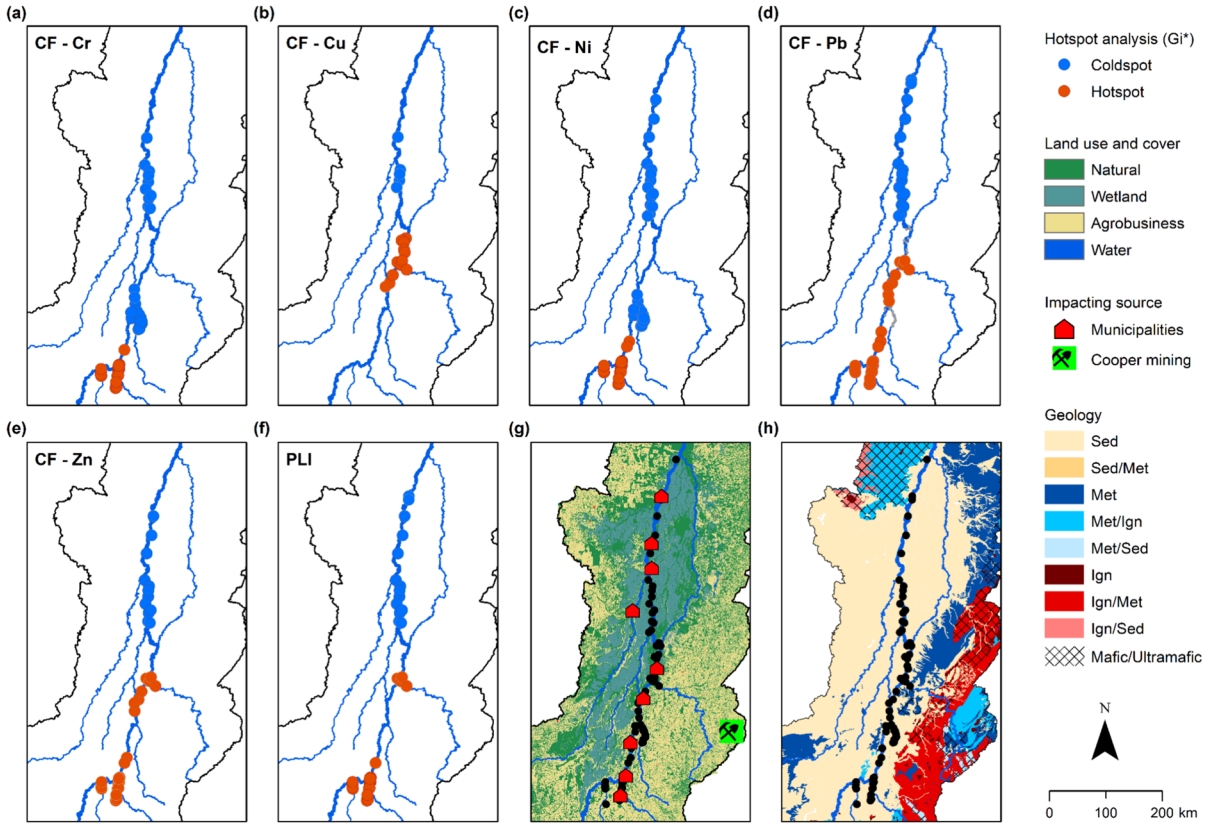

Fig. 3 Hotspot analysis of the contamination factor (CF) of the elements: **a** Cr, **b** Cu, **c** Ni, **d** Pb, **e** Zn, and **f** pollution load index (PLI) considering all elements. **g**, **h** The use and occupation of land and the geology of the study area. On the geological map, the acronyms indicate the rock formation process: Sed, sedimentary rocks, Met, metamorphic rocks, and Ign, igneous rocks. Cross-hatching lines indicate the occurrence of minerals derived from mafic and ultramafic parent material

precise fit between the distance matrix and dendrogram (ccc = 0.986), grouping the elements into three clusters. The first cluster represents Cr; the second cluster represents Zn; and the third cluster represents Pb, Cu, and Ni (Fig. 4b).

The GLMM indicated that the combination of fixed and random effects explained 83% of the variation in Cr concentrations in the bottom sediments. Among the fixed effects (R^2_m = 0.485), Mg concentrations ($R^2_{m\text{-partial}}$ = 0.644), and organic matter content ($R^2_{m\text{-partial}}$ = 0.278) contributed positively to Cr concentrations in the sediments, while the proportion of grassland areas contributed negatively ($R^2_{m\text{-partial}}$ = 0.051) (Fig. 5a).

The GLMM explained 91% of the variation in Cu concentrations, 78% of which was exclusively explained by fixed effects (Fig. 5b). Cu concentrations were negatively influenced by distance to the mining site ($R^2_{m\text{-partial}}$ = 0.101) and by the concentration of phosphorus in the water ($R^2_{m\text{-partial}}$ = 0.063) and positively influenced by the concentration of Mg ($R^2_{m\text{-partial}}$ = 0.656) and the content of organic matter in the sediments ($R^2_{m\text{-partial}}$ = 0.089).

Approximately 88% of the variation in Ni concentration was explained by the GLMM. Among the fixed factors that explained 65% of the total variance, we highlighted the positive influence of Mg concentrations ($R^2_{m\text{-partial}}$ = 0.509), intensity of anthropogenic land use ($R^2_{m\text{-partial}}$ = 0.276), and organic matter content ($R^2_{m\text{-partial}}$ = 0.153). In addition, despite its small explanatory power, the concentration of phosphorus was inversely related to the concentration of Ni in the sediments ($R^2_{m\text{-partial}}$ = 0.061) (Fig. 5c).

The explanatory power of the GLMM, considering Pb as the response variable, was fully attributed to the fixed effects (R^2_c and R^2_m = 0.905). Pb

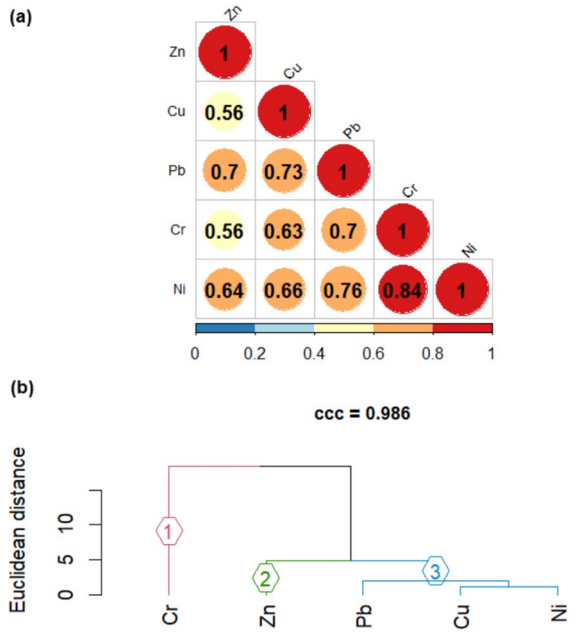

Fig. 4 **a** Spearman's correlation matrix and **b** hierarchical cluster analysis performed using the unweighted pair group method with arithmetic averages (UPGMA). Values in bold indicate significant correlations ($p < 0.05$). ccc, cophenetic correlation coefficient

concentrations were positively influenced by Mg concentration ($R^2_{m\text{-partial}} = 0.368$), organic matter content ($R^2_{m\text{-partial}} = 0.354$), and nitrate concentration in the water ($R^2_{m\text{-partial}} = 0.008$) and negatively influenced by the proportion of wetlands around the lakes ($R^2_{m\text{-partial}} = 0.239$) and phosphorus concentration in the water ($R^2_{m\text{-partial}} = 0.03$) (Fig. 5d). Similarly, the largest proportion of the explanatory power of the Zn model was attributed to fixed effects ($R^2_c = 0.813$, $R^2_m = 0.786$). Zn concentrations were positively influenced by Mg concentrations ($R^2_{m\text{-partial}} = 0.472$) and organic matter content in the sediment ($R^2_{m\text{-partial}} = 0.429$) and negatively influenced by lake depth ($R^2_{m\text{-partial}} = 0.056$) and water turbidity ($R^2_{m\text{-partial}} = 0.018$) (Fig. 5e). Detailed results for each model is presented in Table S6.

Discussion

Geological context and changes in land use and land cover

All PTEs exhibited a strong relationship with Mg concentrations in the sediments, which were used in this study as a proxy for the influence of mafic igneous rocks and metamorphic rocks derived from mafic rocks in the headwaters of the sub-basins. PCA ordination revealed an association between Mg, Fe, and Cr in the bottom sediments (Fig. 2), suggesting weathering of ferromagnesian minerals. In the Itacaiúnas River basin, located near our study area, geochemical anomalies of Ni and Cr in stream sediments have been linked to the presence of mafic and ultramafic rocks (Dall'Agnol et al., 2022; Quaresma et al., 2022; Salomão et al., 2019). This pattern is also reflected in the spatial structure of Ni and Cr concentrations in our study area, which exhibited moderate to strong spatial dependence at a regional scale (> 100 km), confirming the predominant role of endogenous factors, such as the elemental composition of the parental material, in controlling the distribution of these elements in the lakes.

The mean Cr concentration in the lakes of Middle Araguaia was notably higher than that reported in lakes unaffected by significant anthropogenic sources (Carvalho et al., 2018; Sahoo et al., 2019) and in lakes affected by urban (Andrade et al., 2018) and agricultural activities (Rosolen et al., 2015) in other regions of Brazil (Table 3). Globally, the mean Cr concentration was comparable to that determined in lakes in China (Dai et al., 2018; Tao et al., 2012) and India (Nazir et al., 2024), which are impacted by metal mining and smelting, urban effluents, and pesticide application. Additionally, the Cr concentrations were comparable to those measured in Lake Erhai, China, where relatively high concentrations were attributed to the lithogenic origin of the sediments (Yu et al., 2021). In the coastal plain of Pisa, Italy, Amorosi et al. (2013) observed that the weathering of Cr-rich rocks and soils in adjacent river basins (ultramafic provenance) and deposition in floodplain areas were the main factors promoting concentrations of this element above the safety limits established by legislation. McClain and Maher (2016) also demonstrated that the weathering of ultramafic rocks significantly contributes to Cr mobilization into surface

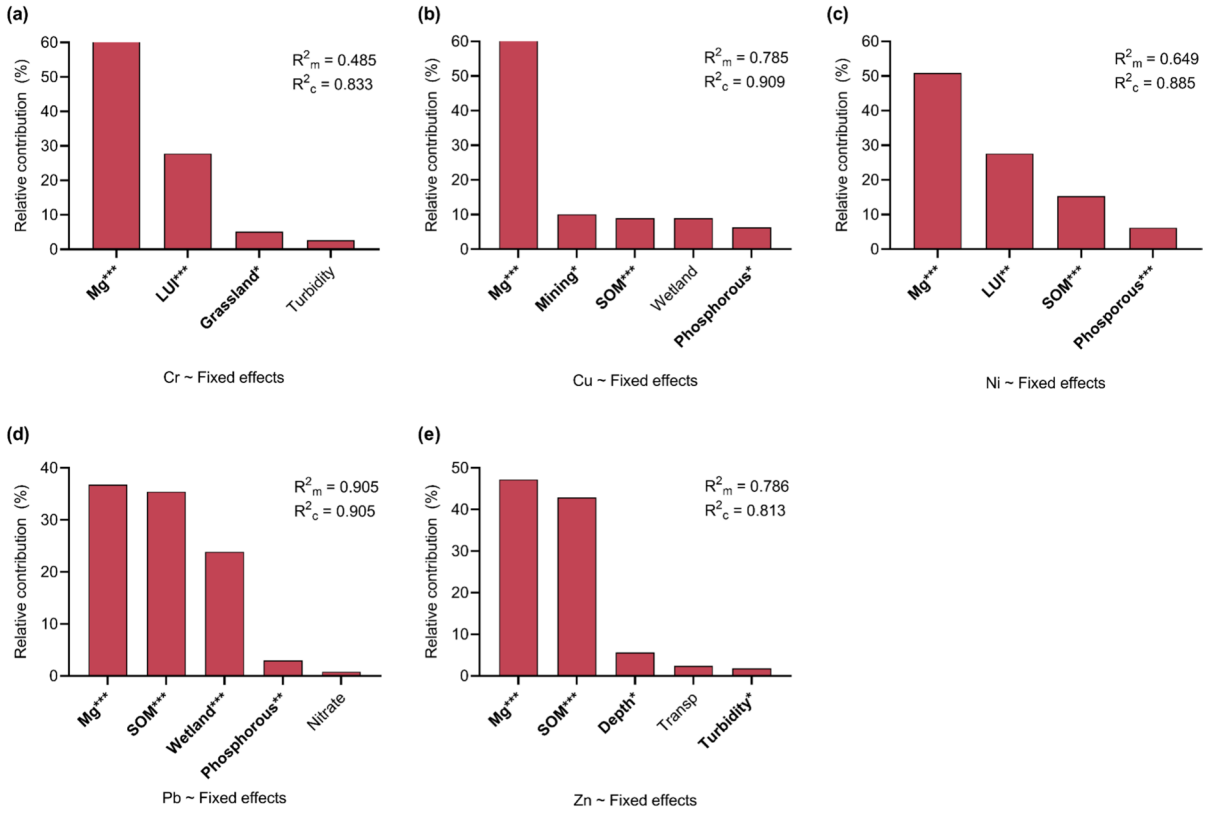

Fig. 5 Relative contribution of fixed effects in each GLMM. **a** Cr. **b** Cu. **c** Ni. **d** Pb. **e** Zn. R^2_c, conditional coefficient of determination (fixed + random effects). R^2_m, marginal coefficient of determination (fixed effects). **Mg**, Mg concentration in the sediment. **SOM**, organic matter content in the sediment. LUI, land use index. The highlighted variables were significant, and the asterisks (*) indicate the level of significance: $p < 0.05$ (*) 0.05; $p < 0.001$ (**); $p < 0.0001$ (***)

waters and depositional environments, such as floodplains, where Cr is primarily transported in its hexavalent form. This aspect is particularly relevant in our study area, where increased land-use intensity has significantly contributed to Cr and Ni accumulation in lake sediments.

Livestock and agriculture are the primary economic activities in the Araguaia River Basin, and approximately half of its area has been converted to these uses over in the last five decades (MapBiomas Project, 2024). Extensive grazing without proper management can significantly affect soil structure and increase bulk density, runoff volumes, and particulate material loads in aquatic ecosystems (Pilon et al., 2017). Thus, changes in land use favor the transport of PTEs to lakes (Monteiro et al., 2023; Ochoa-Contreras et al., 2023). Additionally, the application of phosphate fertilizers is considered a significant source of PTEs derived from agricultural soils to aquatic ecosystems (Tang et al., 2014; Mello et al., 2020; Ustaoğlu, 2021). However, the concentrations of phosphorus and phosphate in the water did not significantly contribute to the variation in the concentrations of PTEs in the bottom sediments. Garnier et al. (2021) observed the colloidal transfer of Cr and Ni bound to iron oxides in the upper layers of soils during precipitation events in the neighboring Niquelândia ultramafic complex (state of Goiás). Thus, soil particles naturally enriched with PTEs may be a source of mobilization in our study area.

The critical sampling sites for Cu, Pb, and Zn contamination in sediments were primarily located in the Crixás-Açú River sub-basin (Fig. 3). Strong correlations between Pb and Cu and between Pb and Zn suggest similarities in terms of the source of mobilization and/or geochemical behavior (Fig. 4a). However, the variographic analysis revealed distinct spatial behaviors (Table S5). Cu

Table 3 Comparison of the total concentrations (mg kg^{-1}) of PTEs (Cr, Cu, Ni, Pb, and Zn) determined in our study in Araguaia with those reported in other lakes located in Brazil and other countries (mean ± standard deviation, minimum–maximum)

Country	Locality	Ecosystem	Cr	Cu	Ni	Pb	Zn	Reference
Brazil	Araguaia floodplain (Brazilian Savanna)	Floodplain lakes	151.9 ± 85.0 22.6–448.7	10.4 ± 7.0 0.7–59.1	15.2 ± 12.5 1.1–92.4	20.9 ± 11.2 1.0–92.4	45.9 ± 15.6 9.5–80.9	This study
Brazil	Puruzinho Lake (Brazilian Amazon)	Floodplain lake	11.8 ± 3.4 6.8–19.3	11.1 ± 3.0 4.1–16.4	Not reported	11.9 ± 2.5 8.2–15.5	66.6 ± 34.6 17.9–113.9	Carvalho et al. (2018)
Brazil	Violão, Amendoim, and Três Irmãs lakes (Brazilian Amazon)	Upland lakes	61.8 ± 30.2 20.0–157.4	30.3 ± 23.7 8.5–222.5	5.7 ± 2.7 1.3–22.1	12.7 ± 7.0 2.8–43.2	31.8 ± 20.2 1.0–135.0	Sahoo et al. (2019)
Brazil	Guaíba Lake (South Region)	Urban lake	38.8 ± 19.0 5.7–74.7	75.8 ± 33.2 13.8–132.1	26.1 ± 10.9 7.8–43.4	30.4 ± 12.2 7.9–53.0	131.1 ± 57.3 32.0–261.0	Andrade et al. (2018)
Brazil	Uberabinha watershed (Southern Region)	Floodplain	68.7 ± 50.6 17.6–155.0	37.8 ± 14.0 15.8–64.6	12.1 ± 4.3 7.0–19.3	12.4 ± 4.7 8.0–20.3	25.5 ± 9.6 15.3–42.6	Rosolen et al. (2015)
Ecuador	Limoncocha Biological Reserve	Marsh lake	36.0 ± 8.8 17.0–48.6	88.0 ± 19.1 54.6–123	21.6 ± 3.7 13.1–27.0	15.1 ± 5.59 5.98–27.7	132 ± 82.5 58.5–376	Carrillo et al. (2022)
China	Taihu Lake	Floodplain lake	147.5 ± 124.1 9.3–464.9	39.6 ± 27.6 16.5–134.6	47.9 ± 23.8 21.2–114.9	40.4 ± 17.2 5.5–69.4	113.2 ± 66.8 24.4–295.9	Tao et al. (2012)
China	Poyang Lake	Floodplain lake	135.9 ± 20.8 96.0–175.2	62.0 ± 20.0 38.1–127.6	Not reported	50.4 ± 14.5 22.5–77.4	132.9 ± 43.7 72.3–254.4	Dai et al. (2018)
China	Erhai Lake	Upland lake	101.6 ± 0.2 58.8–133.0	65.1 ± 0.2 45.1–87.6	57.5 ± 0.2 36.6–77.6	50.2 ± 0.2 35.3–65.8	135.0 ± 0.1 96.0–167.0	Yu et al. (2021)*
India	Dal Lake	Urban lake	139.9 20.8–266.7	57.1 42.3–83.9	98.4 69.6–143.8	10.4 8.1–17.7	105.7 52.4–164.8	Nazir et al. (2024)
Poland	Symsar Lake	Flow-through lake	8.7 ± 1.9	14.6 ± 4.1	26.0 ± 12.6	45.6 ± 21.9	0.11 ± 0.0	Kuriata-Potasznik et al. (2016)
Nigeria	Ologe Lagoon	Lagoon	0.5 ± 0.2	3.5 ± 0.6	0.3 ± 0.4	0.5 ± 0.5	134 ± 34	Ndimele et al. (2024)

*Mean ± coefficient of variation

concentrations exhibited moderate spatial dependence on a regional scale, indicating the influence of regional geology and localized point sources of mobilization. In contrast, Zn concentrations displayed a strong spatial dependence with local-scale variation, predominantly reflecting geological contributions and diffuse mobilization sources. The Cu and Zn concentrations were lower than those reported in lakes affected by urban activities and oil exploration (Andrade et al., 2018; Carrillo et al., 2022) (Table 3). The total Cu concentrations were also lower than those observed in high-altitude

Amazonian lakes associated with mineral deposits from the Carajás Formation (Sahoo et al., 2019).

The Chapada mine is the primary anthropogenic source of Cu in the study area, featuring an open-pit mine and a processing plant designed to process 65,000 tons of Cu sulfide ore (chalcopyrite) daily (Lundin Mining Brasil, 2024). In China, Lin et al. (2022) showed that PTEs from Cu and gold mining in ultramafic rocks exploiting chalcopyrite, magnetite, and pyrrhotite were rapidly diluted downstream (up to 5 km), with Cu and Pb concentrations reaching regional background levels of 19 km (Lin et al., 2022). Despite the potential local-scale impact of mining on Cu concentrations, the mining site was located 45 km from the Crixás-Açú River channel and 150 km upstream of the nearest sampling site. Thus, the inverse relationship between the mining area and Cu concentrations in lake sediments, along with contamination hotspots in the Crixás-Açú subbasin, is likely attributed to Cu mineral deposits (Dai et al., 2018; Salomão et al., 2019). This conclusion is supported by the association between Cu concentrations and rock samples collected from the main channel of the Araguaia River (Fig. 2).

The spatial dependence of Pb concentrations was predominantly attributed to exogenous factors, with variations observed on a regional scale (~ 50 km). Both natural and anthropogenic factors may explain the inverse relationship between Pb concentration and the proportion of flooded areas. The monomodal flood pulse of the Araguaia River results in an active and recent floodplain adjacent to the river channels, with flooding lasting 1–3 months (Irion et al., 2016). This flood period facilitates the input of allochthonous organic and inorganic materials, promoting a reducing environment (Melack & Forsberg, 2001). This process may be intensified in the study area due to high iron concentrations in water during high water periods, altering the reductive dissolution of iron and manganese and mobilizing adsorbed and co-precipitated PTEs in the bottom sediments (Ponting et al., 2021). Therefore, the mobilization of labile Pb in interstitial water under reducing conditions likely contributes to the observed inverse relationship with flooded areas (Chen et al., 2019).

Pb concentrations were below the detection limit in all rock samples, indicating a minimal influence of parental material weathering on the accumulation of Pb in bottom sediments (Table 1). Pb contamination hotspots were identified in the southern floodplain, characterized by intense conversion of native vegetation for agriculture and high tourism potential (Fig. 3). Although the study area lacks significant Pb pollution sources, such as mining or industry, the range of Pb concentrations is comparable to that in urban lakes impacted by wastewater discharge and automobile traffic (Andrade et al., 2018; Kuriata-Potasznik et al., 2016). (Table 3). Inadequate sanitation and solid waste management in the municipalities likely contributed to the diffusion of Pb sources at a local scale. Tourism may exacerbate this issue, as the municipality of Aruanã, located at the confluence of the Vermelho and Araguaia rivers, has a population of 6220 (IBGE, 2022) and receives up to 600,000 tourists annually (Silva et al., 2019). The combination of increased wastewater discharge from tourism and intensified surface runoff in agricultural areas likely enriches PTEs, including Pb, in the bottom sediments (Custodio et al., 2021).

Sediment organic matter and water physicochemical parameters

The organic matter content significantly contributed to the accumulation of PTEs in the sediments, except for Cr. The largest contributions were observed for Zn (43%) and Pb (35%), followed by Ni (15%) and Cu (9%) (Fig. 5). This relationship can be explained by the formation of stable complexes between PTEs and functional groups that comprise organic matter (e.g., carboxyl and amine), which favor adsorption and precipitation in bottom sediments (Khan et al., 2016; Tang et al., 2025). Additionally, the degradation of organic matter in floodplains promotes the formation of sulfides (Hernández-Crespo et al., 2012), increasing the potential for PTE adsorption in sediments (Jean & Bancroft, 1986).

PTEs are predominantly associated with finer fractions of the sediment (silt and clay), whereas sandy sediments have a lower adsorption potential owing to larger pore spaces and smaller surface contact areas (Kissoon et al., 2015). The sediments of the Araguaia River floodplain are sandy and predominantly composed of quartz; hence, organic matter plays a crucial role in the adsorption of PTEs in the bottom sediments (Irion et al., 2016; Monteiro et al., 2024b). In contrast, the absence of an association between Cr concentrations and organic matter content indicates

that PTE is mainly adsorbed in the inorganic fraction of sediments (Kissoon et al., 2015; Stankevica et al., 2020).

The contribution of the physicochemical parameters of water to the environmental distribution of PTEs is inconclusive. The processes of speciation and transport of PTEs depend on the interplay of various physicochemical water parameters, sediment composition, and mobilization sources, making it challenging to establish cause-and-effect relationships between variables (Yao & Gao, 2007). This assertion is supported by the variation in PTE concentrations, which is explained by the intrinsic characteristics of each sub-basin (random effects) and the influence of exogenous factors, as indicated by variographic analysis.

The absence of PTE hotspots on Bananal Island was noteworthy. As an important Ramsar site comprising a mosaic of protected areas, this segment of the Araguaia River exhibits geomorphological characteristics that directly influence physicochemical parameters of water. Although the Araguaia River carries high loads of suspended sediments, the Bananal Island segment has lower altitudes and a lower degree of channel confinement, resulting in greater sandbank formation and reduced sediment transport (Suizu et al., 2023). Consequently, lakes situated on Bananal Island exhibit greater water transparency, indicating a reduction in the transport of PTEs associated with particulate matter into these lakes.

Potential risks of PTEs contamination for biological communities and human health

Field studies have shown that multiple taxa of microorganisms, particularly Cr, Ni, and Cu, exhibit negative correlations with PTE concentrations in bottom sediments. This suggests that certain taxa exhibit low resistance to these PTEs (Chen et al., 2018; Ni et al., 2016). In a study by Ni et al. (2016), impacts on biological communities were noted despite the low concentrations of available metals in the samples. Therefore, the total concentrations of PTEs can indicate the potential impact on biological communities, whereas the bioavailable fraction reflects the direct effect on biota (Ni et al., 2016). A mesocosm study found that total Cu concentrations within the range observed in our study (46 mg kg^{-1}) can significantly alter the composition of sediment microbial communities (Sutcliffe et al., 2019). Similarly, concentrations of Cr, Cu, Ni, and Pb in the range determined in our study were positively correlated with the inhibition of germination and root growth in the aquatic plant *Lepidium sativum* (Tarnawski & Baran, 2018).

The accumulation of PTEs in bottom sediments can also negatively affect organisms at higher trophic levels. In the Cerrado biome, the contamination of a stream with Cr-rich agricultural compounds leads to a decline in the richness and diversity of benthic macroinvertebrates (Silva & Corbi, 2023). Notably, the mean total Cr concentration reported by Silva et al. (2023) was four times lower than that observed in our study (38.4 ± 11.3 mg kg^{-1}). In the Ebro River basin, Spain, Pb, Cr, and Ni concentrations within the range detected in our study negatively affected macroinvertebrate and diatom community compositions (Roig et al., 2016). However, Roig et al. (2016) determined different degrees of bioavailability among PTEs, with higher bioavailable fractions for Ni, while Cr and Pb were mainly associated with organic matter and Fe and Mn oxyhydroxides, respectively. The strong correlation between PTEs observed in our study (Fig. 4) suggests that physiological processes in macroinvertebrates may intensify the co-occurrence and bioaccumulation of these elements (Arnold et al., 2021). Indeed, ecotoxicological tests have indicated that the combination of PTEs in bottom sediments significantly impacts mortality rates and inhibits the growth of ostracods (Mata et al., 2020). Consequently, the PTE concentrations in the Araguaia River lakes could affect the composition of the biological community.

DelValls et al. (1998) observed that concentrations of PTEs in sediments, including Cr, Cu, and Pb, caused histological damage in juvenile fish *Sparus aurata*. Based on ecotoxicological tests, the authors indicated that Cr concentrations above 90 mg kg^{-1} could have deleterious effects on fish (DelValls et al., 1998). Onita et al. (2021) reported significant correlations between PTE concentrations and histopathological lesions in the gills, kidneys, and liver of fish with different feeding habits. Additionally, PTE accumulation in bottom sediments and biological communities can have direct implications for human health. In Lake Puruzinho (Brazilian Amazon), although the average Cr concentration in bottom sediments was an order of magnitude lower than that in our study (Carvalho et al., 2018; Table 3), exposure to Cr

through fish consumption poses health risks (Nascimento et al., 2022). A similar pattern was observed for Pb exposure via fish consumption (Azevedo et al., 2023), where the average Pb concentration in sediments was half that recorded in Araguaia River lakes (Carvalho et al., 2018; Table 3). Subsequent studies (Azevedo-Silva et al., 2023; Waichman et al., 2025) demonstrated that the highest PTE concentrations, and consequently the greatest risk of human exposure through fish consumption, were found in iliophagous and detritivorous species, which primarily forage in bottom sediments. This highlights the role of sediment as a critical source of PTEs entering the trophic chain. Furthermore, in floodplain environments, fluctuations in the hydrological regime can facilitate PTE mobilization into the water column through dissolution (Wade et al., 2025) and resuspension (Chen et al., 2024), leading to bioaccumulation at the base of the food web.

Although the Cr concentrations were predominantly above the sediment quality guidelines, only three lakes exhibited significant contamination levels, underscoring the need to establish regional background concentrations for accurate contamination assessments (Wang et al., 2019). Indeed, Cr and Ni concentrations in watersheds with soils derived from mafic rocks often exceed the regulatory thresholds (Amorosi et al., 2014; Begum et al., 2015). It is important to note that in addition to total concentrations, the bioavailability of PTEs must be considered when assessing risk (Sammartino, 2004). Chromium occurs in rocks mainly in its trivalent form; however, once accumulated in anoxic sediments, which is characteristic of floodplains, natural Cr (III) is oxidized by Mn into Cr (IV) (Ao et al., 2022). Although a large part of Cr (VI) remains bound to the solid phase through adsorption and precipitation (Botsou et al., 2022), it is the most abundant form of Cr in the surface and groundwater (Fantoni et al., 2002; Kazakis et al., 2015; Kaprara et al., 2015). Thus, even when these elements originate from natural sources, their mobilization and transformation in aquatic ecosystems can pose risks to biological communities and human health.

Conclusions

Most lakes in the Araguaia River floodplain exhibit significant integrated enrichment of potentially toxic elements (PTEs) (PLI >1), with a predominantly low to moderate degree of individual contamination. Notably, Ni and Cr showed the highest proportions of samples with moderate to significant enrichment, accompanied by a considerable to very high degree of contamination. The total concentration of Cr exceeded the limits set by the sediment quality guidelines in 98.6% of the lakes. The critical areas for PTE accumulation are in the sub-basins of the Água Limpa Stream and the Vermelho River, which are regions characterized by intense land use and the presence of igneous and metamorphic rocks in the headwaters. The distinct elemental compositions of the rocks collected from the main channel of the Araguaia River and the bottom sediments of the lakes confirm the role of parental material weathering from the headwaters in the accumulation of PTEs in the downstream floodplain lakes. Conversely, lakes with the lowest probability of contamination are situated on Bananal Island, which comprises a mosaic of conservation units and indigenous lands, underscoring the importance of legally protected natural areas in maintaining the ecological integrity of floodplains.

The moderate to strong correlation among all PTEs suggests a common source of mobilization. However, the results from hierarchical cluster analysis (HCA) and generalized linear mixed models (GLMM) indicate that different factors influence the accumulation of PTEs in lakes. All PTEs showed a strong relationship with the Mg concentrations in the sediments. Anthropogenic land-use intensity positively influenced Cr and Ni concentrations in the sediments, likely due to the transport of soil particles naturally enriched with these PTEs. Organic matter content significantly contributed to the accumulation of PTEs in the sediments (except for Cr), particularly Zn and Pb, likely due to the formation of stable complexes between the PTEs and functional groups within the organic matter. In contrast, Cr appeared to be primarily adsorbed into the inorganic fraction of sediments.

Our results provide valuable information regarding the sources and distribution of PTEs in the Araguaia River floodplain. However, our study has two limitations. Despite the high explanatory power of GLMMs, we did not conduct a complete

physicochemical characterization of the bottom sediments. In addition to the organic matter content, grain size and the quantification of Fe, Mn, and Al oxides could provide important information on the transport and accumulation of PTEs in the floodplain. Additionally, given the relatively high concentrations of Cr determined in this study and the potential risks to human health from exposure to Cr (IV), the speciation of Cr in sediment samples would provide more accurate information on exposure risks. Future studies should conduct robust physicochemical characterization of the sediment samples, in addition to evaluating Cr concentrations and speciation in various environmental compartments, including surface waters.

Acknowledgements This study was carried out as part of the "Araguaia Vivo 2030" research program. The authors thank the National Institute of Science and Technology (INCT) in Ecology, Evolution, and Biodiversity Conservation for financial and logistical support during sample collection, and the "Expedição Araguaia Vivo 2023" team for collecting the sediment samples, especially Bruno Rhanniery Batista dos Santos, Jocilaine Santos de Jesus, and Thaís Sampaio Silva. We also thank Ygor Oliveira Sarmento Rodrigues for collecting the rock samples and his work preparing the sediment samples, João Pedro Rudrigues de Souza for preparing the rock samples, and Professor Priscilla de Carvalho for providing the water nutrient data.

Author contribution LCM: Conceptualization, Methodology, Formal analysis, Investigation, Writing—Original Draft, Visualization. LCGV: Conceptualization, Methodology, Writing—Original Draft, Resources, Supervision, Project administration, Funding acquisition. JVEB: Conceptualization, Methodology, Formal analysis, Writing—Original Draft, Resources. TAMP: Investigation. WACJ: Investigation. WPS: Investigation. LAGS: Investigation. JFGJ: Resources, Writing—Review & Editing, Funding acquisition. JCN: Formal analysis, Resources, Writing—Review & Editing. JAFDF: Formal analysis, Writing—Review & Editing, Funding acquisition. JG: Resources, Writing—Review & Editing. CLF: Investigation. RA: Methodology, Resources, Writing—Review & Editing. WRB: Methodology, Resources, Writing—Review & Editing. All the authors reviewed the final version of the manuscript.

Funding This study was authorized by the Instituto Chico Mendes de Conservação da Biodiversidade (ICMBio) and received financial support from: (i) Fundação de Apoio à Pesquisa do Distrito Federal (FAPDF) (proc. no. 00193–00001567/2021–80, and proc. no. 00193–00000308/2023–1); (ii) Fundo Brasileiro para a Biodiversidade (FUNBIO), Instituto Humanize, and Eurofins Foundation (Programa de Bolsas FUNBIO 2021; proc. no. 017/2022); (iii) Project Sustainable Development and Biodiversity Conservation of the Tocantins-Araguaia Hydrographic Basin (project 25) Public Call no. 01/2021 SNSH-MDR sponsored by Banco Itaú and executed by Tropical Water Research Alliance (TWRA); (iii) National Institute of Science and Technology (INCT) in Ecology, Evolution, and Biodiversity Conservation funded by Conselho Nacional de Desenvolvimento Científico e Tecnológico (CNPq) (grant 465610/2014–5) and Fundação de Amparo à Pesquisa do Estado de Goiás (FAPEG) (grant 201810267000023); (iv) "Araguaia Vivo 2030" research program, supported by TWRA and FAPEG (conv. P&D&I TWRA/FAPEG 03/2023, proc. no. 202210267000536), and PPBio Araguaia, supported by Conselho Nacional de Desenvolvimento Científico e Tecnológico (CNPq) (proc. no. 441114/2023–7); and (v) Conselho Nacional de Desenvolvimento Científico e Tecnológico (CNPq) (proc. no. 408035/2021–8, and proc. no. 407888/2021–7). LCM was supported by a CNPq PhD scholarship. LCGV, JFGJ, JCN, JAFDF, JG, and WRB were supported by CNPq research grants.

Data availability Data will be made available on reasonable request.

Declarations

Competing interests The authors declare no competing interests.

References

Alloway, B. J. (1990). *Heavy metal in soils*. John Wiley and Sons.

Amorosi, A., Guermandi, M., Marchi, N., & Sammartino, I. (2014). Fingerprinting sedimentary and soil units by their natural metal contents: A new approach to assess metal contamination. *Science of the Total Environment, 500*, 361–372. https://doi.org/10.1016/j.scitotenv.2014.08.078

Amorosi, A., Sammartino, I., & Sarti, G. (2013). Background levels of potentially toxic metals from soils of the Pisa coastal plain (Tuscany, Italy) as identified from sedimentological criteria. *Environmental Earth Sciences, 69*, 1661–1671. https://doi.org/10.1007/s12665-012-2001-8

Andrade, L. C., Tiecher, T., de Oliveira, J. S., Andreazza, R., Inda, A. V., & de Oliveira Camargo, F. A. (2018). Sediment pollution in margins of the Lake Guaíba, Southern Brazil. *Environmental Monitoring and Assessment, 190*, 1–13. https://doi.org/10.1007/s10661-017-6365-9

Angelini, M. E., Heuvelink, G. B., Kempen, B., & Morrás, H. J. (2016). Mapping the soils of an Argentine Pampas region using structural equation modelling. *Geoderma, 281*, 102–118. https://doi.org/10.1016/j.geoderma.2016.06.031

Ao, M., Sun, S., Deng, T., Zhang, F., Liu, T., Tang, Y., ... & Qiu, R. (2022). Natural source of Cr (VI) in soil: The anoxic oxidation of Cr (III) by Mn oxides. *Journal of Hazardous Materials*, *433*, 128805. https://doi.org/10.1016/j.jhazmat.2022.128805

APHA - American Public Health Association. (2005). *Standard methods for the examination of water and wastewater* (21st ed.). American Public Health Association/

American Water Works Association/Water Environment Federation.

Aquino, S., Latrubesse, E. M., & de Souza Filho, E. E. (2009). Caracterização hidrológica e geomorfológica dos afluentes da Bacia do Rio Araguaia. *Revista Brasileira de Geomorfologia*, *10*(1). https://doi.org/10.20502/rbg.v10i1.116

Arnold, A., Murphy, J. F., Pretty, J. L., Duerdoth, C. P., Smith, B. D., Rainbow, P. S., ... & Jones, J. I. (2021). Accumulation of trace metals in freshwater macroinvertebrates across metal contamination gradients. *Environmental Pollution*, *276*, 116721. https://doi.org/10.1016/j.envpol.2021.116721

Azevedo, S. M., do Nascimento, L. S., de Oliveira Silva, L., de Almeida, M. G., Azevedo, L. S., Constantino, W. D., ... & Pestana, I. A. (2023). Flood pulse as a driving force of Pb variation in four fish guilds from Puruzinho Lake (western Amazon). *Environmental Science and Pollution Research*, *30*(13), 38728-38737. https://doi.org/10.1007/s11356-022-25015-z

Azevedo-Silva, C. E., Pizzochero, A. C., Galvão, P. M., Ometto, J. P., de Camargo, P. B., Azeredo, A., ... & Dorneles, P. R. (2023). Trophic dynamics of methylmercury and trace elements in a remote Amazonian Lake. *Environmental Research*, *237*, 116889. https://doi.org/10.1016/j.envres.2023.116889

Basti, S., Sahu, C., Dash, P. K., Pati, S. S., & Sahu, S. K. (2025). Sediment heavy metal speciation of Hirakud Reservoir—a Ramsar site in Mahanadi River in India. *Environmental Monitoring and Assessment, 197*, 417. https://doi.org/10.1007/s10661-025-13898-7

Begum, S., Shah, M. T., Muhammad, S., & Khan, S. (2015). Role of mafic and ultramafic rocks in drinking water quality and its potential health risk assessment, Northern Pakistan. *Journal of Water and Health, 13*(4), 1130–1142. https://doi.org/10.2166/wh.2015.066

Boës, X., Rydberg, J., Martinez-Cortizas, A., Bindler, R., & Renberg, I. (2011). Evaluation of conservative lithogenic elements (Ti, Zr, Al, and Rb) to study anthropogenic element enrichments in lake sediments. *Journal of Paleolimnology, 46*, 75–87. https://doi.org/10.1007/s10933-011-9515-z

Botsou, F., Koutsopoulou, E., Andrioti, A., Dassenakis, M., Scoullos, M., & Karageorgis, A. P. (2022). Chromium speciation, mobility, and Cr (VI) retention–release processes in ultramafic rocks and Fe–Ni lateritic deposits of Greece. *Environmental Geochemistry and Health, 44*(8), 2815–2834. https://doi.org/10.1007/s10653-021-01078-8

Brazil. (2012). *Resolução CONAMA n° 454, de 1º de novembro de 2012*. Retrivied July 20, 2024, from https://www.icmbio.gov.br/cepsul/legislacao/resolucao/236-2012.html

Cambardella, C. A., Moorman, T. B., Novak, J. M., Parkin, T. B., Karlen, D. L., Turco, R. F., & Konopka, A. E. (1994). Field-scale variability of soil properties in central Iowa soils. *Soil Science Society of America Journal, 58*(5), 1501–1511. https://doi.org/10.2136/sssaj1994.03615995005800050033x

Carrillo, K. C., Rodríguez-Romero, A., Tovar-Sánchez, A., Ruiz-Gutiérrez, G., & Fuente, J. R. V. (2022). Geochemical baseline establishment, contamination level and ecological risk assessment of metals and As in the Limoncocha lagoon sediments, Ecuadorian Amazon region. *Journal of Soils and Sediments*, 1–23. https://doi.org/10.1007/s11368-021-03084-w

Carvalho, D. P. D., Almeida, R. D., Manzatto, Â. G., Freitas, O. B. D., & Bastos, W. R. (2018). Dynamics of metals in lacustrine sediments: Case study of the Madeira River, Amazon region. *Revista Brasileira De Recursos Hídricos, 23*, e21. https://doi.org/10.1590/2318-0331.231820170026

Carvalho, M. A. R., Botero, W. G., & de Oliveira, L. C. (2022). Natural and anthropogenic sources of potentially toxic elements to aquatic environment: A systematic literature review. *Environmental Science and Pollution Research, 29*(34), 51318–51338. https://doi.org/10.1007/s11356-022-20980-x

CCME - Canadian Council of Ministers of the Environment. (2003). *Canadian water quality guidelines for the protection of aquatic life: Inorganic mercury and methylmercury*. Retrivied July 20, 2024, from https://publications.gc.ca/site/eng/9.558456/publication.html

Chen, X. P., Chen, H. Y., Sun, J., Zhang, X., He, C. Q., Liu, X. Y., ... & Väänänen, K. (2018). Shifts in the structure and function of the microbial community in response to metal pollution of fresh water sediments in Finland. *Journal of Soils and Sediments*, *18*, 3324–3333. https://doi.org/10.1007/s11368-017-1782-5

Chen, M., Ding, S., Lin, J., Fu, Z., Tang, W., Fan, X., ... & Wang, Y. (2019). Seasonal changes of lead mobility in sediments in algae-and macrophyte-dominated zones of the lake. *Science of the Total Environment*, *660*, 484–492. https://doi.org/10.1016/j.scitotenv.2019.01.010

Chen, J., Liu, M., Wang, F., Ding, Y., Fan, D., & Wang, H. (2024). Accumulation and migration of particulate trace metals by artificial flood event of the Yellow River: From Xiaolangdi reservoir to estuary. *Science of the Total Environment, 912*, 168614. https://doi.org/10.1016/j.scitotenv.2023.168614

CPRM - Serviço Geológico do Brasil. (2004). Mapeamento Geológico do Brasil. Retrivied July 11, 2024, from https://www.sgb.gov.br/

Custodio, M., Fow, A., Chanamé, F., Orellana-Mendoza, E., Peñaloza, R., Alvarado, J. C., ... & Pizarro, S. (2021). Ecological risk due to heavy metal contamination in sediment and water of natural wetlands with tourist influence in the central region of Peru. *Water*, *13*(16), 2256. https://doi.org/10.3390/w13162256

Dai, L., Wang, L., Li, L., Liang, T., Zhang, Y., Ma, C., & Xing, B. (2018). Multivariate geostatistical analysis and source identification of heavy metals in the sediment of Poyang Lake in China. *Science of the Total Environment, 621*, 1433–1444. https://doi.org/10.1016/j.scitotenv.2017.10.085

Dale, M. R. T., & Fortin, M. J. (2014). *Spatial analysis: A guide for ecologists* (2nd ed.). Cambridge University Press.

Dall'Agnol, R., Sahoo, P. K., Salomão, G. N., de Araújo, A. D. M., da Silva, M. S., Powell, M. A., ... & Guilherme, L. R. G. (2022). Soil-sediment linkage and trace element contamination in forested/deforested areas of the Itacaiúnas River Watershed, Brazil: To what extent land-use change

plays a role?. *Science of the Total Environment*, *828*, 154327. https://doi.org/10.1016/j.scitotenv.2022.154327

DelValls, T. A., Blasco, J., Sarasquete, M. C., Forja, J. M., & Gómez-Parra, A. (1998). Evaluation of heavy metal sediment toxicity in littoral ecosystems using juveniles of the FishSparus aurata. *Ecotoxicology and Environmental Safety, 41*(2), 157–167. https://doi.org/10.1006/eesa.1998.1680

Dong, Y., Lu, H., & Lin, H. (2024). Comprehensive study on the spatial distribution of heavy metals and their environmental risks in high-sulfur coal gangue dumps in China. *Journal of Environmental Sciences, 136*, 486–497. https://doi.org/10.1016/j.jes.2022.12.023

Donohue, I., & Garcia Molinos, J. (2009). Impacts of increased sediment loads on the ecology of lakes. *Biological Reviews, 84*(4), 517–531. https://doi.org/10.1111/j.1469-185X.2009.00081.x

Fantoni, D., Brozzo, G., Canepa, M., Cipolli, F., Marini, L., Ottonello, G., & Zuccolini, M. (2002). Natural hexavalent chromium in groundwaters interacting with ophiolitic rocks. *Environmental Geology, 42*, 871–882. https://doi.org/10.1007/s00254-002-0605-0

Ferreira, S. L., da Silva Junior, J. B., dos Santos, I. F., de Oliveira, O. M., Cerda, V., & Queiroz, A. F. (2022). Use of pollution indices and ecological risk in the assessment of contamination from chemical elements in soils and sediments–Practical aspects. *Trends in Environmental Analytical Chemistry, 35*, e00169. https://doi.org/10.1016/j.teac.2022.e00169

Garnier, J., Quantin, C., Raous, S., Guimarães, E., & Becquer, T. (2021). Field availability and mobility of metals in Ferralsols developed on ultramafic rock of Niquelândia, Brazil. *Brazilian Journal of Geology, 51*(01), e20200092. https://doi.org/10.1590/2317-4889202120200092

Getis, A., spsampsps Ord, J. K. (2010). The analysis of spatial association by use of distance statistics. In L. Anselin, spsampsps S. Rey (Eds), *Perspectives on spatial data analysis. Advances in spatial science* (pp. 127–145). Springer, Berlin, Heidelberg. https://doi.org/10.1007/978-3-642-01976-0_10

Goovaerts, P. (1997). *Geostatistics for natural resources evaluation*. Oxford University Press.

Hakanson, L. (1980). An ecological risk index for aquatic pollution control. A sedimentological approach. *Water Research, 14*(8), 975–1001. https://doi.org/10.1016/0043-1354(80)90143-8

Hanfi, M. Y., Mostafa, M. Y., & Zhukovsky, M. V. (2020). Heavy metal contamination in urban surface sediments: Sources, distribution, contamination control, and remediation. *Environmental Monitoring and Assessment, 192*, 1–21. https://doi.org/10.1007/s10661-019-7947-5

Hernández-Crespo, C., Martín, M., Ferrís, M., & Oñate, M. (2012). Measurement of acid volatile sulphide and simultaneously extracted metals in sediment from Lake Albufera (Valencia, Spain). *Soil and Sediment Contamination: An International Journal, 21*(2), 176–191. https://doi.org/10.1080/15320383.2012.649374

IARC - International Agency for Research on Cancer. (2012). *IARC Monographs on the evaluation of risk to humans: Volume 100C*. Retrivied July 26, 2024, from https://monographs.iarc.who.int/monographs-available/

IBGE - Instituto Brasileiro de Geografia e Estatística. (2022). Censo Demográfico 2022. Retrivied July 11, 2024, from https://censo2022.ibge.gov.br

Irion, G., Nunes, G. M., Nunes-da-Cunha, C., de Arruda, E. C., Santos-Tambelini, M., Dias, A. P., ... & Junk, W. J. (2016). Araguaia river floodplain: Size, age, and mineral composition of a large tropical savanna wetland. *Wetlands*, *36*, 945–956. https://doi.org/10.1007/s13157-016-0807-y

Jean, G. E., & Bancroft, G. M. (1986). Heavy metal adsorption by sulphide mineral surfaces. *Geochimica Et Cosmochimica Acta, 50*(7), 1455–1463. https://doi.org/10.1016/0016-7037(86)90319-4

Junk, W. J., Piedade, M. T. F., Lourival, R., Wittmann, F., Kandus, P., Lacerda, L. D., ... & Agostinho, A. A. (2014). Brazilian wetlands: Their definition, delineation, and classification for research, sustainable management, and protection. *Aquatic Conservation: Marine and Freshwater Ecosystems*, *24*(1), 5–22. https://doi.org/10.1002/aqc.2386

Kapoor, D., & Singh, M. P. (2021). Heavy metal contamination in water and its possible sources. In A. Sharma., V. Kumar, & A. Cerda (Eds.), *Heavy metals in the environment: Impact, assessment, and remediation* (pp. 179–189). Elsevier. https://doi.org/10.1016/B978-0-12-821656-9.00010-9

Kaprara, E., Kazakis, N., Simeonidis, K., Coles, S., Zouboulis, A. I., Samaras, P., & Mitrakas, M. (2015). Occurrence of Cr (VI) in drinking water of Greece and relation to the geological background. *Journal of Hazardous Materials, 281*, 2–11. https://doi.org/10.1016/j.jhazmat.2014.06.084

Kazakis, N., Kantiranis, N., Voudouris, K. S., Mitrakas, M., Kaprara, E., & Pavlou, A. (2015). Geogenic Cr oxidation on the surface of mafic minerals and the hydrogeological conditions influencing hexavalent chromium concentrations in groundwater. *Science of the Total Environment, 514*, 224–238. https://doi.org/10.1016/j.scitotenv.2015.01.080

Khan, B., Ullah, H., Khan, S., Aamir, M., Khan, A., & Khan, W. (2016). Sources and contamination of heavy metals in sediments of Kabul River: The role of organic matter in metals retention and accumulation. *Soil and Sediment Contamination: An International Journal, 25*(8), 891–904. https://doi.org/10.1080/15320383.2016.1224226

Kissoon, L. T. T., Jacob, D. L., Hanson, M. A., Herwig, B. R., Bowe, S. E., & Otte, M. L. (2015). Multi-elements in waters and sediments of shallow lakes: Relationships with water, sediment, and watershed characteristics. *Wetlands, 35*, 443–457. https://doi.org/10.1007/s13157-015-0632-8

Kou, Y., Zhang, W., Zhang, Y., Ge, X., & Wu, Y. (2024). Toxic effects of trace metal (loid) mixtures on aquatic organisms. *Science of The Total Environment*, 174677. https://doi.org/10.1016/j.scitotenv.2024.174677

Kumar, A., Kumar, A., MMS, C. P., Chaturvedi, A. K., Shabnam, A. A., Subrahmanyam, G., ... & Yadav, K. K. (2020). Lead toxicity: Health hazards, influence on food chain, and sustainable remediation approaches. *International Journal of Environmental Research and Public*

Health, *17*(7), 2179. https://doi.org/10.3390/ijerph17072179

Kuriata-Potasznik, A., Szymczyk, S., Skwierawski, A., Glińska-Lewczuk, K., & Cymes, I. (2016). Heavy metal contamination in the surface layer of bottom sediments in a flow-through lake: A case study of Lake Symsar in Northern Poland. *Water, 8*(8), 358. https://doi.org/10.3390/w8080358

Latrubesse, E. M., Amsler, M. L., de Morais, R. P., & Aquino, S. (2009). The geomorphologic response of a large pristine alluvial river to tremendous deforestation in the South American tropics: The case of the Araguaia River. *Geomorphology, 113*(3–4), 239–252. https://doi.org/10.1016/j.geomorph.2009.03.014

Latrubesse, E. M., & Stevaux, J. C. (2002). Geomorphology and environmental aspects of the Araguaia fluvial basin, Brazil. *Zeitschrift Für Geomorphologie. Supplementband, 129*, 109–127.

Li, H., Wang, J., Zhao, B., Gao, M., Shi, W., Zhou, H., ... & He, J. (2018). The role of major functional groups: Multi-evidence from the binding experiments of heavy metals on natural fulvic acids extracted from lake sediments. *Ecotoxicology and Environmental Safety*, *162*, 514–520. https://doi.org/10.1016/j.ecoenv.2018.07.038

Li, Z., Li, X., Wang, S., Che, F., Zhang, Y., Yang, P., ... & Fu, Z. (2023). Adsorption and desorption of heavy metals at water sediment interface based on Bayesian model. *Journal of Environmental Management*, *329*, 117035. https://doi.org/10.1016/j.jenvman.2022.117035

Li, Y., Zhou, H., Gao, B., & Xu, D. (2021). Improved enrichment factor model for correcting and predicting the evaluation of heavy metals in sediments. *Science of the Total Environment, 755*, 142437. https://doi.org/10.1016/j.scitotenv.2020.142437

Lima-Junior, D. P., Lima, L. B., Carnicer, C., Zanella, R., Prestes, O. D., Floriano, L., & Júnior, P. D. M. (2024). Exploring the relationship between land-use and pesticides in freshwater ecosystem: A case study of the Araguaia River Basin, Brazil. *Environmental Advances, 15*, 100497. https://doi.org/10.1016/j.envadv.2024.100497

Lin, C. Y., Ali, B. N. M., Tair, R., Musta, B., Abdullah, M. H., Cleophas, F., ... & Yusoff, I. (2022). Distance impacts toxic metals pollution in mining affected river sediments. *Environmental Research*, *214*, 113757. https://doi.org/10.1016/j.envres.2022.113757

Lipp, A. G., Roberts, G. G., Whittaker, A. C., Gowing, C. J., & Fernandes, V. M. (2020). River sediment geochemistry as a conservative mixture of source regions: Observations and predictions from the Cairngorms, UK. *Journal of Geophysical Research: Earth Surface, 125*(12), e2020JF005700. https://doi.org/10.1029/2020JF005700

López, D. L., Gierlowski-Kordesch, E., & Hollenkamp, C. (2010). Geochemical mobility and bioavailability of heavy metals in a lake affected by acid mine drainage: Lake Hope, Vinton County, Ohio. *Water, Air, & Soil Pollution, 213*, 27–45. https://doi.org/10.1007/s11270-010-0364-6

Lundin Mining Brasil. (2024). *Operação*. Retrivied July 20, 2024, from https://lundinmining.com.br/operacao

MapBiomas Project. (2024). *Coleção 5 da Série Anual de Mapas de Uso e Cobertura da Terra do Brasil*. Retrivied April 15, 2024, from http://mapbiomas.org

Mata, H. K., Al Salah, D. M. M., Ngweme, G. N., Konde, J. N., Mulaji, C. K., Kiyombo, G. M., & Poté, J. W. (2020). Toxic metal concentration and ecotoxicity test of sediments from dense populated areas of Congo River, Kinshasa, Democratic Republic of the Congo. *Environmental Chemistry and Ecotoxicology, 2*, 83–90. https://doi.org/10.1016/j.enceco.2020.07.001

McClain, C. N., & Maher, K. (2016). Chromium fluxes and speciation in ultramafic catchments and global rivers. *Chemical Geology, 426*, 135–157. https://doi.org/10.1016/j.chemgeo.2016.01.021

Melack, J., & Forsberg, B. (2001). Biochemistry of Amazon floodplain lakes and associated wetlands. In M. E. McClain, R. Victoria, & J. E. Richey (Eds.), *The Biogeochemistry of the Amazon Basin* (pp. 235–274). Oxford University Press, Oxford. https://doi.org/10.1093/oso/9780195114317.003.0017

Mello, F. M., Teodoro, M. E. L., Mesquita, G. N., Pinheiro, H. S. K., & Bilal, E. (2020). Heavy metals backgrounds and guiding values in southwestern amazonian soils–A comparative study. *Carpathian Journal of Earth and Environmental Sciences*, *15*(1). https://doi.org/10.26471/cjees/2020/015/110

Monteiro, L. C., Vieira, L. C. G., Bernardi, J. V. E., de Castro Moraes, L., Rodrigues, Y. O. S., de Souza, J. P. R., ... & Dórea, J. G. (2023). Ecological risk of mercury in bottom sediments and spatial correlation with land use in Neotropical savanna floodplain lakes, Araguaia River, Central Brazil. *Environmental Research*, *238*, 117231. https://doi.org/10.1016/j.envres.2023.117231

Monteiro, L. C., Vieira, L. C. G., Bernardi, J. V. E., Rodrigues, Y. O. S., de Mesquita, L. P. B., Souza, J. P. R. D., ... & Bastos, W. R. (2024a). Mercury bioconcentration and translocation in rooted macrophytes (Paspalum repens Berg.) from floodplain lakes in the Araguaia River Watershed, Brazilian Savanna. *Water*, *16*(9), 1199. https://doi.org/10.3390/w16091199

Monteiro, L. C., Vieira, L. C. G., Bernardi, J. V. E., Bastos, W. R., de Souza, J. P. R., do Nascimento Recktenvald, M. C. N., ... & de Souza, J. R. (2024b). Local and landscape factors influencing mercury distribution in water, bottom sediment, and biota from lakes of the Araguaia River floodplain, Central Brazil. *Science of the Total Environment*, *908*, 168336. https://doi.org/10.1016/j.scitotenv.2023.168336

Moraes, L., Bernardi, J. V. E., de Souza, J. P. R., Portela, J. F., Vieira, L. C. G., Sousa Passos, C. J., ... & Dorea, J. G. (2023). Sediment mercury, geomorphology and land use in the Middle Araguaia River Floodplain (Savanna Biome, Brazil). *Soil Systems*, *7*(4), 97. https://doi.org/10.3390/soilsystems7040097

Nascimento, L. S., de Oliveira Silva, L., de Azevedo, S. M., de Almeida, R., Almeida, M. G., Azevedo, L. S., ... & Pestana, I. A. (2022). Spatial-temporal dynamics of Cr in fish from Puruzinho Lake (Western Amazon) and dietary risk assessment. *Chemosphere*, *300*, 134576. https://doi.org/10.1016/j.chemosphere.2022.134576

Nazir, A., Hussain, S. M., Riyaz, M., Kere, Z., Zargar, M. A., & Karun, D. L. K. (2024). Environmental risk assessment, spatial distribution, and abundance of heavy metals in surface sediments of Dal Lake-Kashmir, India. *Environmental Advances, 17*, 100562. https://doi.org/10.1016/j.envadv.2024.100562

Ndimele, P. E., et al. (2024). Source apportionment, ecological and health risk assessment of potentially toxic elements in water, sediment and blackchin tilapia {Sarotherodon melanotheron (Rüppell 1852)} from Lagos and Ologe Lagoons, Lagos State, Nigeria. *Journal of Trace Elements and Minerals, 9*, 100173. https://doi.org/10.1016/j.jtemin.2024.100173

Ni, C., Horton, D. J., Rui, J., Henson, M. W., Jiang, Y., Huang, X., & Learman, D. R. (2016). High concentrations of bioavailable heavy metals impact freshwater sediment microbial communities. *Annals of Microbiology, 66*, 1003–1012. https://doi.org/10.1007/s13213-015-1189-8

Ochoa-Contreras, R., Jara-Marini, M. E., Ruiz-Fernández, A. C., Sanchez-Cabeza, J. A., Meza-Figueroa, D., & Pérez-Bernal, L. H. (2023). Historical fluxes of metal and metalloids in an aquatic ecosystem affected by land-use change and mining activities in northwestern Mexico. *International Journal of Sediment Research, 38*(5), 724–738. https://doi.org/10.1016/j.ijsrc.2023.05.003

Onita, B., Albu, P., Herman, H., Balta, C., Lazar, V., Fulop, A., ... & Dinischiotu, A. (2021). Correlation between heavy metal-induced histopathological changes and trophic interactions between different fish species. *Applied Sciences*, *11*(9), 3760. https://doi.org/10.3390/app11093760

Pelicice, F. M., Agostinho, A. A., Akama, A., Andrade Filho, J. D., Azevedo-Santos, V. M., Barbosa, M. V. M., ... & Zuanon, J. (2021). Large-scale degradation of the Tocantins-Araguaia River basin. *Environmental Management*, *68*, 445–452. https://doi.org/10.1007/s00267-021-01513-7

Pilon, C., Moore Jr, P. A., Pote, D. H., Pennington, J. H., Martin, J. W., Brauer, D. K., ... & Lee, J. (2017). Long-term effects of grazing management and buffer strips on soil erosion from pastures. *Journal of Environmental Quality*, *46*(2), 364–372. https://doi.org/10.2134/jeq2016.09.0378

Plach, J. M., Elliott, A. V., Droppo, I. G., & Warren, L. A. (2011). Physical and ecological controls on freshwater floc trace metal dynamics. *Environmental Science & Technology, 45*(6), 2157–2164. https://doi.org/10.1021/es1031745

Ponting, J., Kelly, T. J., Verhoef, A., Watts, M. J., & Sizmur, T. (2021). The impact of increased flooding occurrence on the mobility of potentially toxic elements in floodplain soil–A review. *Science of the Total Environment, 754*, 142040. https://doi.org/10.1016/j.scitotenv.2020.142040

Quaresma, L. S., Silva, G. D. S. E., Sahoo, P. K., Salomão, G. N., & Dall'Agnol, R. (2022). Source apportionment of chemical elements and their geochemical baseline values in surface water of the Parauapebas river basin, southeast Amazon, Brazil. *Minerals, 12*(12), 1579. https://doi.org/10.3390/min12121579

R Core Team. (2024). *R: A language and environment for statistical computing*. R Foundation for Statistical Computing, Vienna, Austria. https://www.R-project.org/

Rawer-Jost, C., Zenker, A., & Böhmer, J. (2004). Reference conditions of German stream types analysed and revised with macroinvertebrate fauna. *Limnologica, 34*(4), 390–397. https://doi.org/10.1016/S0075-9511(04)80008-2

Reimann, C., Filzmoser, P., & Garrett, R. G. (2005). Background and threshold: Critical comparison of methods of determination. *Science of the Total Environment, 346*(1–3), 1–16. https://doi.org/10.1016/j.scitotenv.2004.11.023

Roig, N., Sierra, J., Moreno-Garrido, I., Nieto, E., Gallego, E. P., Schuhmacher, M., & Blasco, J. (2016). Metal bioavailability in freshwater sediment samples and their influence on ecological status of river basins. *Science of the Total Environment, 540*, 287–296. https://doi.org/10.1016/j.scitotenv.2015.06.107

Rosolen, V., De-Campos, A. B., Govone, J. S., & Rocha, C. (2015). Contamination of wetland soils and floodplain sediments from agricultural activities in the Cerrado Biome (State of Minas Gerais, Brazil). *Catena, 128*, 203–210. https://doi.org/10.1016/j.catena.2015.02.007

Ruello, M. L., Sani, D., Sileno, M., & Fava, G. (2011). Persistence of heavy metals in river sediments. *Chemistry and Ecology, 27*(S1), 13–19. https://doi.org/10.1080/02757540.2010.534985

Sadeghi, S. H. R., Harchegani, M. K., & Younesi, H. A. (2012). Suspended sediment concentration and particle size distribution, and their relationship with heavy metal content. *Journal of Earth System Science, 121*, 63–71. https://doi.org/10.1007/s12040-012-0143-4

Sahoo, P. K., Dall'Agnol, R., Salomão, G. N., Junior, J. D. S. F., Silva, M. S., e Souza Filho, P. W. M., ... & Siqueira, J. O. (2019). High resolution hydrogeochemical survey and estimation of baseline concentrations of trace elements in surface water of the Itacaiúnas River Basin, southeastern Amazonia: Implication for environmental studies. *Journal of Geochemical Exploration*, *205*, 106321. https://doi.org/10.1016/j.gexplo.2019.06.003

Salomão, G. N., Figueiredo, M. A., Dall'Agnol, R., Sahoo, P. K., de Medeiros Filho, C. A., da Costa, M. F., & Angélica, R. S. (2019). Geochemical mapping and background concentrations of iron and potentially toxic elements in active stream sediments from Carajás, Brazil–implication for risk assessment. *Journal of South American Earth Sciences, 92*, 151–166. https://doi.org/10.1016/j.jsames.2019.03.014

Sammartino, I. (2004). Heavy-metal anomalies and bioavailability from soils of southeastern Po Plain. *GeoActa, 3*, 35–42.

Sigel, H., & Sigel, A. (2019). The bio-relevant metals of the periodic table of the elements. *Zeitschrift Für Naturforschung B, 74*(6), 461–471. https://doi.org/10.1515/znb-2019-0056

Silva, B. N. C., & Corbi, J. J. (2023). Aquatic macroinvertebrate community structure affected by chromium contamination in the Monte Alegre Stream (SP): A historical comparative case study. *Brazilian Archives of Biology and Technology, 66*, e23220117. https://doi.org/10.1590/1678-4324-2023220117

Silva, L. G., de Lima, S. C., & Nazareno, E. (2019). O povo Karajá de Aruanã-GO/Brasil: Turismo, território e vida indígena. *Tempos Históricos, 23*(1), 216–240.

Sojka, M., Jaskuła, J., Barabach, J., Ptak, M., & Zhu, S. (2022). Heavy metals in lake surface sediments in protected areas in Poland: Concentration, pollution, ecological risk, sources and spatial distribution. *Scientific Reports, 12*(1), 15006. https://doi.org/10.1038/s41598-022-19298-y

Sokal, R. R., Oden, N. L., & Thomson, B. A. (1998). Local spatial autocorrelation in biological variables. *Biological Journal of the Linnean Society, 65*(1), 41–62. https://doi.org/10.1006/bijl.1998.0238

Stankevica, K., Vincevica-Gaile, Z., Klavins, M., Kalnina, L., Stivrins, N., Grudzinska, I., & Kaup, E. (2020). Accumulation of metals and changes in composition of freshwater lake organic sediments during the Holocene. *Chemical Geology, 539*, 119502. https://doi.org/10.1016/j.chemgeo.2020.119502

Suizu, T. M., Latrubesse, E. M., & Bayer, M. (2023). Geomorphic diversity of the middle Araguaia River, Brazil: A segment-scale classification to support river management. *Journal of South American Earth Sciences, 121*, 104166. https://doi.org/10.1016/j.jsames.2022.104166

Sutcliffe, B., Hose, G. C., Harford, A. J., Midgley, D. J., Greenfield, P., Paulsen, I. T., & Chariton, A. A. (2019). Microbial communities are sensitive indicators for freshwater sediment copper contamination. *Environmental Pollution, 247*, 1028–1038. https://doi.org/10.1016/j.envpol.2019.01.104

Sutherland, R. A. (2000). Bed sediment-associated trace metals in an urban stream, Oahu, Hawaii. *Environmental Geology, 39*, 611–627. https://doi.org/10.1007/s002540050473

Swaroop, A., Bagchi, M., Preuss, H. G., Zafra-Stone, S., Ahmad, T., & Bagchi, D. (2019). Benefits of chromium (III) complexes in animal and human health. In J. B. Vincent (Eds.), *The nutritional biochemistry of chromium (III)* (pp. 251–278). Elsevier. https://doi.org/10.1016/B978-0-444-64121-2.00008-8

Tang, W., Ao, L., Zhang, H., & Shan, B. (2014). Accumulation and risk of heavy metals in relation to agricultural intensification in the river sediments of agricultural regions. *Environmental Earth Sciences, 71*, 3945–3951. https://doi.org/10.1007/s12665-013-2779-z

Tang, W., Sun, L., Zhu, Y., Ng, J. C., Huang, J., Xu, Z., & Zhang, H. (2025). Difference analysis of organic matter-mediated heavy metal pollution in the sediments of urban water bodies. *Science of the Total Environment, 968*, 178747. https://doi.org/10.1016/j.scitotenv.2025.178747

Tao, Y., Yuan, Z., Wei, M., & Xiaona, H. (2012). Characterization of heavy metals in water and sediments in Taihu Lake, China. *Environmental Monitoring and Assessment, 184*, 4367–4382. https://doi.org/10.1007/s10661-011-2270-9

Tarnawski, M., & Baran, A. (2018). Use of chemical indicators and bioassays in bottom sediment ecological risk assessment. *Archives of Environmental Contamination and Toxicology, 74*(3), 395–407. https://doi.org/10.1007/s00244-018-0513-2

Teixeira, A. S., Vieira, L. C. G., de Souza, C. A., Bernardi, J. V. E., & Monteiro, L. C. (2024). Evidence of water surface and flow reduction in the main hydrographic basin of the Brazilian savannah (Cerrado biome): The Araguaia river. *Hydrobiologia, 851*(10), 2503–2518. https://doi.org/10.1007/s10750-024-05471-z

Tepe, Y., Şimşek, A., Ustaoğlu, F., & Taş, B. (2022). Spatial–temporal distribution and pollution indices of heavy metals in the Turnasuyu Stream sediment, Turkey. *Environmental Monitoring and Assessment, 194*(11), 818. https://doi.org/10.1007/s10661-022-10490-1

Tomlinson, D. L., Wilson, J. G., Harris, C. R., & Jeffrey, D. W. (1980). Problem in heavy metals in estuaries and the formation of pollution index. *Helgol Wiss Meeresunlter, 33*(1–4), 566–575.

U.S. Environmental Protection Agency. (1996). Method 3050B, Revision 1, December 1996, Final update IIIB, acid digestion of sludges, solids and soils, methods, and soils, part of test methods for evaluating solid waste, physical/chemical methods, in: USEPA (Ed.), *3000 Series: Inorganic Sample Preparation*. U.S. Environmental Protection Agency slide 1 of 3 Test Your, Washington, D.C, pp. 1–12.

Ustaoğlu, F. (2021). Ecotoxicological risk assessment and source identification of heavy metals in the surface sediments of Çömlekci stream, Giresun, Turkey. *Environmental Forensics, 22*(1–2), 130–142. https://doi.org/10.1080/15275922.2020.1806148

Ustaoğlu, F. & Islan, M. S. (2020). Potential toxic elements in sediment of some rivers at Giresun, Northeast Turkey: A preliminary assessment for ecotoxicological status and health risk. *Ecological Indicators, 113*, 106237. https://doi.org/10.1016/j.ecolind.2020.106237

van Griethuysen, C., Luitwieler, M., Joziasse, J., & Koelmans, A. A. (2005). Temporal variation of trace metal geochemistry in floodplain lake sediment subject to dynamic hydrological conditions. *Environmental Pollution, 137*(2), 281–294. https://doi.org/10.1016/j.envpol.2005.01.023

Vandeuren, A., Pereira, B., Kaba, A. J., Titeux, H., & Delmelle, P. (2023). Environmental bioavailability of arsenic, nickel and chromium in soils impacted by high geogenic and anthropogenic background contents. *Science of the Total Environment, 902*, 166073. https://doi.org/10.1016/j.scitotenv.2023.166073

Wade, A. M., Eckley, C. S., Noerpel, M., Goetz, J., Leptich, D., Prestbo, K., ... & Luxton, T. P. (2025). Mobilization of porewater Pb and Zn in response to seasonal wetting and drying within contaminated floodplains. *Science of The Total Environment*, *958*, 178053. https://doi.org/10.1016/j.scitotenv.2024.178053

Waichman, A. V., de Souza Nunes, G. S., de Oliveira, R., López-Heras, I., & Rico, A. (2025). Human health risks associated to trace elements and metals in commercial fish from the Brazilian Amazon. *Journal of Environmental Sciences, 148*, 230–242. https://doi.org/10.1016/j.jes.2023.12.029

Wang, J., Liu, G., Lu, L., Zhang, J., & Liu, H. (2015). Geochemical normalization and assessment of heavy metals (Cu, Pb, Zn, and Ni) in sediments from the Huaihe River, Anhui, China. *Catena, 129*, 30–38. https://doi.org/10.1016/j.catena.2015.02.008

Wang, S., Wang, W., Chen, J., Zhao, L., Zhang, B., & Jiang, X. (2019). Geochemical baseline establishment and

pollution source determination of heavy metals in lake sediments: A case study in Lihu Lake, China. *Science of the Total Environment, 657*, 978–986. https://doi.org/10.1016/j.scitotenv.2018.12.098

Yao, Z., & Gao, P. (2007). Heavy metal research in lacustrine sediment: A review. *Chinese Journal of Oceanology and Limnology, 25*(4), 444–454. https://doi.org/10.1007/s00343-007-0444-7

Yu, Z., Liu, E., Lin, Q., Zhang, E., Yang, F., Wei, C., & Shen, J. (2021). Comprehensive assessment of heavy metal pollution and ecological risk in lake sediment by combining total concentration and chemical partitioning. *Environmental Pollution, 269*, 116212. https://doi.org/10.1016/j.envpol.2020.116212

Yuan, X., Zhang, L., Li, J., Wang, C., & Ji, J. (2014). Sediment properties and heavy metal pollution assessment in the river, estuary and lake environments of a fluvial plain, China. *Catena, 119*, 52–60. https://doi.org/10.1016/j.catena.2014.03.008

Zhang, Y., Yu, J., Su, Y., Du, Y., & Liu, Z. (2019). Long-term changes of water quality in aquaculture-dominated lakes as revealed by sediment geochemical records in Lake Taibai (Eastern China). *Chemosphere, 235*, 297–307. https://doi.org/10.1016/j.chemosphere.2019.06.179